Received: 9 April 2018 | Revised: 20 July 2018 | Accepted: 23 July 2018 | Published on: 29 August 2018

DOI: 10.1002/joc.5820

International Journal of Climatology RMetS

RESEARCH ARTICLE

Propagation of climate model biases to biophysical modelling can complicate assessments of climate change impact in agricultural systems

De Li Liu[1,2] | Bin Wang[1] | Jason Evans[2] | Fei Ji[3] | Cathy Waters[4] | Ian Macadam[2,3] | Xihua Yang[3] | Kathleen Beyer[3]

[1]NSW Department of Primary Industries, Wagga Wagga Agricultural Institute, Wagga Wagga, NSW 2650, Australia

[2]Climate Change Research Centre and ARC Centre of Excellence for Climate Extremes, University of New South Wales, Sydney, New South Wales, Australia

[3]New South Wales Office of Environment and Heritage, Department of Planning and Environment, Sydney, NSW 1232, Australia

[4]NSW Department of Primary Industries, Orange Agricultural Institute, Orange, NSW 2800, Australia

Correspondence
De Li Liu, NSW Department of Primary Industries, Wagga Wagga Agricultural Institute, Wagga Wagga, NSW 2650, Australia.
Email: de.li.liu@dpi.nsw.gov.au

Funding information
NSW Office of Environment and Heritage (OEH), Grant/Award Number: RDE959; NSW Department of Primary Industries

Regional climate model (RCM) simulations are being increasingly used for climate change impact assessments, but their application is challenging due to considerable biases inherited from global climate model (GCM) simulations and generated from dynamical downscaling processes. This study assesses the biases in NARCliM (NSW and ACT regional climate modelling) simulations and quantifies the consequence of the climate biases in the downstream assessment of climate change impact on wheat crop system, using the Agricultural Production System sIMulator (APSIM). Results showed that post-processing bias-corrected temperature and rainfall data from NARCliM had small annual mean biases but large biases in the crop growing season (CGS). During the CGS, the mean bias error of rainfall was generally positive for rainfall probability and negative for intensity, which subsequently resulted in APSIM simulating negative biases for runoff and deep drainage and positive bias in soil evaporation. Bias in soil water balance and water availability resulted in less plant transpiration and less N uptake, ultimately, leading to large negative biases in crop yields. A simple bias correction of the simulated crop yield driven by RCMs could result in a largely consistent distribution with those generated with APSIM simulations forced by observed climate. Our results showed that RCM simulation biases could confound with the climate change signal and produced an unreliable estimate of the effects of the changes in climate and farm management variables on crop yields. The results suggested that RCM simulations with the current bias correction on the RCM-simulated outputs applied on an annual basis were inadequate for climate change assessments which involve biophysical models. Our study highlights the need for improved RCM simulations by eliminating the systemic biases associated with rainfall characteristics, although suitable post-processing bias correction on a seasonal or monthly basis may result in improved RCM simulations for agricultural impacts of climate change.

KEYWORDS
APSIM, bias correction, bias propagation, bio-physical crop model, NARCliM, rainfall intensity, rainfall probability, RCMs, wheat cropping system

1 | INTRODUCTION

The assessment of climate change impacts on crop productivity often involves evaluating the outputs from crop simulation models under various crop management practice as well as different climate scenarios (Ruiz-Ramos and Mínguez, 2010; Vanuytrecht *et al.*, 2014; Anwar *et al.*, 2015; Donatelli *et al.*, 2015; Wiebe *et al.*, 2015; Wang *et al.*, 2017). Biophysical-based models represent the physiological processes of crop development as a response to climate and environmental variables. They are able to simulate daily interactions with the climate, atmospheric CO_2 concentration ([CO_2]), soils and management practice that determine crop growth and production. Many agricultural models require input data that describes the environmental conditions at high spatial and temporal resolution (Ruiz-Ramos *et al*., 2016; Cammarano *et al*., 2017). Information about future climate conditions often comes from atmosphere–ocean global climate models (GCMs), which attempt to represent the full global climate system and simulate the response of the system to assumed scenarios for emissions of greenhouse gases and aerosols onto the atmosphere. However, the use of projected climate data from GCMs to drive crop models is challenging as the GCM grid size is much larger than that required for crop modelling. Regional/local-scale detail must be added through spatial downscaling (Ramarohetra *et al*., 2015).

Dynamical downscaling by regional climate models (RCMs) is often applied to bridge the gap between coarse-resolution GCM data and high-resolution climate data that can be used to drive biophysical models at a regional or site-specific scale (Macadam *et al*., 2016). RCMs explicitly account for many physical processes such as orographic features, coastal boundaries and spatially more detailed depictions of gradients within the atmosphere than GCMs (Fowler *et al*., 2007; Yin *et al*., 2011). However, RCMs inherit biases from GCMs and generate biases from dynamical downscaling processes, which are referred for any discrepancy of interest between a model output characteristic and the "truth" (Ehret *et al*., 2012). The biases in RCM simulations are themselves an additional source of uncertainty for downstream crop modelling. For example, when Pascal *et al*. (2011) applied different RCMs outputs to drive the SARRA-H crop model in Senegal over the 1990–2000 period, they found large differences in the simulated wheat yields depending on the RCM used and that a change in the physical parameterizations of a single RCM can lead to a large dispersion in crop yield simulations. Moreover, Ramarohetra *et al*. (2015) showed that the bias in the simulated crop yield strongly depends on the choices in the RCM setup, the choice of the land surface model being of primary importance in their study. Glotter *et al*. (2014) found that although the RCMs correct some GCM biases related to fine-scale geographic features, the use of a RCM cannot compensate for broad-scale systematic errors that dominate the errors for simulated maize yields when using two RCMs and the DSSAT-CERES-maize crop model over the United States. These large biases may seriously overestimate or underestimate simulated changes. Therefore, for the assessment of climate effects on crop yield, bias correction of climate variables or crop yield is a necessary procedure in the application of the RCM output as well as the output from statistical downscaling methods (Bakker *et al*., 2014; Yang *et al*., 2014).

With the growing interest in regional climate projections, the NSW Office of Environment and Heritage in conjunction with the University of New South Wales and other partners developed the NSW and ACT regional climate modelling (NARCliM) project (Evans *et al*., 2014) that resulted in 12 RCMs available for three 20-year time slices (1990–2009 for baseline, 2020–2039 for 2030s and 2060–2070 for 2070s). The NARCliM RCM simulations of southeast Australia had a horizontal resolution of ~10 km and captured the spatial pattern of temperature and rainfall better than the driving GCMs (Olson *et al*., 2016b). However, overall, the RCMs tended to have cold and wet bias when compared to climate observations. Furthermore, comparisons between NARCliM RCM simulations driven by re-analysis data and gauge or AWAP (Australian Water Availability Project) observations suggested that the RCMs used by NARCliM did not agree perfectly with observed rainfall and did not produce the spatial distribution of the observed rainfall correctly (Manage *et al*., 2016). Evans *et al*. (2017) applied a quantile mapping bias correction to the climate model outputs, based on theoretical distribution functions, and found the bias correction was successful in removing a large proportion of the bias in extreme rainfall, but unsuccessful in correcting biases in the length of maximum wet and dry spells. The post bias corrected NARCliM simulations have become available and have been widely used in climate change impact assessments in eastern Australia (Ji *et al*., 2015; Olson *et al*., 2016a; Fita *et al*., 2017). For example, Yang *et al*. (2016a) applied the NARCliM outputs for assessing climate change impacts on water erosion across NSW and found rainfall erosivity and hillslope erosion risk were projected to increase by approximately 7 and 19% in 2030s and 2070s over the baseline, respectively. Ji *et al*. (2018) reported that the frequency of suitable snowmaking conditions for the Australian Alps in both 2030s and 2070s was substantially decreased compared to the baseline (1990–2009). However, these studies often simply compared modelled outputs derived from the climate of future periods with the baseline. The assessment of percentage change can be particularly problematic as the biases in RCM simulations can alter the magnitude of climate change impacts.

As agricultural crops are sensitive to climate and environmental variations (Lobell and Burke, 2010), agricultural models are built to represent the biophysical processes that require realistic climate data as inputs. It is therefore crucial to quantify the errors inevitably propagated by downscaling techniques through combined climate-crop modelling. The NARCliM projections are an outstanding tool for investigating the effect of using RCMs on simulated yields in eastern Australia, one of the most vulnerable areas to climate change. However, to our knowledge, very few studies have addressed the response of crop simulations to errors and uncertainties in the NARCliM data set. In this study, we therefore used NARCliM simulations to drive a crop model and assessed the simulated attributes of a wheat cropping system compared to the simulations driven by historical observed climate. The specific objectives were (a) to assess the biases in NARCliM simulations related crop growth stages, (b) to determine the effects of climate biases on crop simulation modelling outputs, (c) to quantify the consequence of climate biases on climate change impact assessment and (d) to apply a simple bias correction method to the outputs of the biophysical model to reduce the uncertainty of the climate change impact assessment. The underlying hypothesis is that if the climate variables simulated by RCMs were realistic and perfectly matched the observed climate, the outputs of a biophysical model forced by the observed and RCMs projected climate should be identical.

2 | MATERIAL AND METHODS

2.1 | Study domain

The domain of this study is the Murray-Riverina cropping (MRC) region, southern New South Wales (Figure 1), Australia, covering an area of 125,551 km^2. The region is characterized by a semi-arid climate with minimum temperature of 9.3 °C, maximum temperature of 22.0 °C and long-term annual rainfall of 495 mm. A total of 370 historical observed weather sites in the region and 56 soil types registered in APSoil (https://www.apsim.info/Products/APSoil.aspx) are located for the region. The most frequently occurring soil textures from the region were sandy clay and, sandy loam above a clay layer, while the soil types range from Sodosols to Kandosols (Isbell, 2016). The soil type nearest to the respective climate site was used to run the crop model.

2.2 | Climate data

The observed climate variables (daily minimum temperature, maximum temperature, rainfall and solar radiation) in 370 sites for the 20-year NARCliM baseline period (1990–2009) were downloaded from the SILO-patched point data set (Jeffrey *et al*., 2001).

The remaining climate data for this study were derived from the NARCliM ensemble of regional climate projections. This provided detailed regional climate projections for southeast Australia by downscaling outputs from a selection of the CMIP3 GCMs. Data from a subsequent generation of GCMs, the CMIP5 GCMs, has since become available, but the NARCliM projections remain the most detailed comprehensive climate projections for NSW. In NARCliM, four GCMs, namely CCCMA3.1, CSIRO-MK3.0, ECHAM5 and MIROC3.2 (abbreviated as CC, CS, EC and MI, respectively) were selected from the Coupled Model Intercomparison Project phase 3 (CMIP3) ensemble. GCM simulations of the SRES A2 emission scenario (business as usual scenario, in terms of the energy imbalance of the climate system, similar to currently used representative concentration pathway [RCP] 8.5) were used (Table 1). The selection of the GCMs was based on model performance over Australia, independence of errors, and to span the full range of potential future climates over southeastern Australia (Evans *et al*., 2014). The selected four GCMs were used to drive three structurally different RCM configurations to form a 12-member GCM-RCM ensemble, hereafter denoted as 12 RCM simulations (Table 1). The three RCM configurations (referred to as R1, R2 and R3 hereafter) were variants of the WRF V3.3 model (Skamarock *et al*., 2005) with three different physics scheme combinations (Table 1). As described in the RCM selection process (Evans *et al*., 2014), WRF is a modelling framework within which one builds models. By choosing different physics scheme combinations within WRF different RCMs, possessing different error characteristics and even climate sensitivity can create different RCMs that enable to sample uncertainties associated with dynamical downscaling. The three RCMs were specifically selected from 36 combinations considering eight typical east coast low events (which is a major climate driver for southeast Australia). Performance of RCMs and independence of RCMs were considered in the selection. These three RCMs performed well in terms of their ability to reproduce observations of the east coast low events and were somewhat independent in the sense that

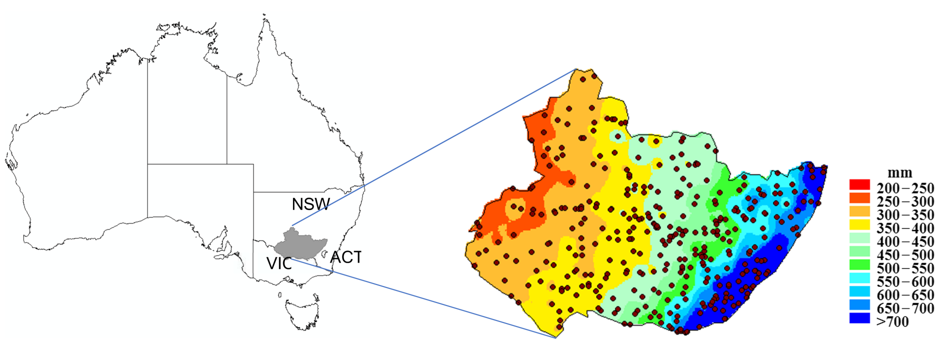

FIGURE 1 The baseline observed annual rainfall (1990–2009) and the distribution of the 370 observed climate sites in the MRC region [Colour figure can be viewed at wileyonlinelibrary.com]

TABLE 1 The 12 RCM configurations from the selected four GCMs and three ensemble members of WRF v3.3 model with different physics scheme combinations. The GCMs projected changes in rainfall and temperature were based on the far future period (2060–2079) relative to the baseline period (1990–2009) for NARCliM land domain

	GCMs			WRF V3.3 model				
		Projected change						
RCM-GCM code	GCM name	Rainfall	Temperature	NARCliM ensemble member	Planetary boundary layer physics/surface layer physics	Cumulus physics	Micro-physics	Short/longwave radiation physics
CC-R1				R1	MYJ/Eta similarity	KF	WDM 5 class	Dudhia/RRTM
CC-R2	CCCMA3.1	Wetter	Hotter	R2	MYJ/Eta similarity	BMJ	WDM 5 class	Dudhia/RRTM
CC-R3				R3	YSU/MM5 similarity	KF	WDM 5 class	CAM/CAM
CS-R1				R1	MYJ/Eta similarity	KF	WDM 5 class	Dudhia/RRTM
CS-R2	CSIRO-MK3.0	Drier	Warmer	R2	MYJ/Eta similarity	BMJ	WDM 5 class	Dudhia/RRTM
CS-R3				R3	YSU/MM5 similarity	KF	WDM 5 class	CAM/CAM
EC-R1				R1	MYJ/Eta similarity	KF	WDM 5 class	Dudhia/RRTM
EC-R2	ECHAM5	Drier	Hotter	R2	MYJ/Eta similarity	BMJ	WDM 5 class	Dudhia/RRTM
EC-R3				R3	YSU/MM5 similarity	KF	WDM 5 class	CAM/CAM
MI-R1				R1	MYJ/Eta similarity	KF	WDM 5 class	Dudhia/RRTM
MI-R2	MIROC3.2	Wetter	Warmer	R2	MYJ/Eta similarity	BMJ	WDM 5 class	Dudhia/RRTM
MI-R3				R3	YSU/MM5 similarity	KF	WDM 5 class	CAM/CAM

biases between the simulations and observations differed between the three RCMs (Evans *et al*., 2012; Evans *et al*., 2014; Ji *et al*., 2014).

For each of the 370 study sites, climate data for the three 20-year NARCliM time slices (1990–2009, 2030–2039 and 2060–2079) were extracted from the nearest grid point of the bias-corrected 10 km NARCliM simulations. This post-processing bias correction used a quantile matching technique as described in Piani *et al*. (2010) that allowed correction of the full distribution of daily precipitation, maximum and minimum temperatures. First, Gamma distributions were fitted to the observed and modelled daily precipitation time series, and Gaussian distributions to the observed and modelled daily maximum and minimum temperature time series. Corrections were then applied to allow the fitted distributions of daily RCM output to match the fitted distributions of daily observations. The AWAP observations (Jones *et al*., 2009) for period 1990–2009 were used to calculate the corrections. These corrections were assumed to be independent of future climate change and the same corrections were also applied respectively to the future precipitation and temperature values. Due to unavailable radiation data in the AWAP data set, the post-processing bias correction was not applied to radiation.

2.3 | Agricultural biophysical modelling

2.3.1 | The APSIM model

Agricultural Production Systems sIMulator (APSIM) is a biophysical model that was designed to simulate agricultural systems at a field scale and the model has been widely validated for different environments worldwide including the study region (Keating *et al*., 2003; Holzworth *et al*., 2014; O'Leary *et al*., 2016). In this study, APSIM version 7.7 under various farming treatments were forced by observed climate (SILO) data and NARCliM data (i.e., 12 RCM simulations). APSIM considers the response of the cropping system to soil properties (mainly soil water and nitrogen), climate (radiation, temperature, rainfall and [CO_2]) and management practices, including cultivar selection, sowing date (SD) decision, irrigation options, nitrogen fertilization, tillage operations and residue management. APSIM simulated the plant response to changing [CO_2] via effects on plant radiation use efficiency, transpiration efficiency and critical leaf nitrogen concentration. As the responses in these parameters are functions of [CO2], we calculated [CO_2] for each year using the empirical function of Yang *et al*. (2014, eq. 2),

$$[CO_2]_y = 2641 + \frac{0.098139 \times y - 211.71}{3.5566 \times y^{-0.37996} - 0.19123}, \quad (1)$$

where y is the calendar year from 1900 to 2100 (i.e., y = 1900, 1901, …, 2100).

The details of APSIM settings and key parameters implemented are described in Liu *et al*. (2017).

2.3.2 | APSIM set up

To test the responses of wheat cropping system to uncertainties in climate variables under different agronomical managements, we ran APSIM under two contrasting crop residue incorporations (residue removal with no tillage, denoted as RI0%, and 100% residue incorporations with three tillages, denoted as RI100%) and two N-applications (55 and 165 kg/ha, denoted as N55 and N165, respectively). The combination of the residue incorporation and N-application resulted in four treatments, that is, RI0N55, RI0N165, RI100N55 and RI100N165. This would allow simulating the interaction of cropping systems between climate and farming management activities.

The sowing date (SD) of the crop was set automatically using a "sowing rule" designed to represent common farm management practices. With large spatial variation in soil and climate across the MRC region, we needed to develop a suitably flexible sowing rule. To set a sowing rule suited to all soils and rainfall conditions across the entire region, we considered sowing as a function of soil water (SW) content, plant available water capacity (PAWC), recent rainfall and day of year in the season. We used the conditions given in Equation (2a) to determine SD occurring the first day when this condition was met,

$$\mathrm{CR}_4 \geq (\mathrm{CR}_o + a)\left(\frac{\mathrm{PAWC}}{\mathrm{PAWC}+\mathrm{SW}}\right)^3 - a, \quad (2a)$$

where CR_0 is the amount of cumulative rainfall in previous 4 days at SW =0 and varied with day of year (d) and a is also a function of d, which are calculated by

$$\mathrm{CR}_0 = \frac{4320}{d-36},\ a = \frac{600.04}{d-37.13}. \quad (2b)$$

The constants were determined so that sowing on dry soil (SW =0) required a total of 58 and 30 mm of CR_0 on d = 111 and 181 for the starting and ending of sowing widow (April 21 to June 30), whereas dry sowing (no recent rain) can be performed when SW = PAWC. Here, we used this innovative approach to determine SD based on soil water content and cumulative rainfall and crops sown in dry soils when a large amount of rainfall occurs in the most recent days or sown in wet soils requiring no rainfall or small amount of recent rainfall, hence the sowing rule suits a wide range of conditions.

To assess the application of nitrogen across the region and climate effects on the cropping system without carry over of cumulative effects, we reset the soil water and nitrogen to their respective initial level on February 1 in each year.

2.4 | Biases and secondary bias correction

We defined the NARCliM climate biases as the difference between the average values (X_M) in the NARCliM data set and their respectively observed values (X_O). Similarly, the biases in APSIM-simulated outputs are the difference between the APSIM-simulated outputs forced by RCMs (X_M) and those forced by observed climate (X_O). We defined mean bias error (MBE) as the difference in the mean over the 20-year period either in absolute terms (e.g., temperature in °C, run off in mm) or in percentage (e.g., rainfall, %) using the formula of

$$\mathrm{MBE} = \overline{X}_M - \overline{X}_O \text{ or } \mathrm{MBE}(\%) = 100 \times \frac{\overline{X}_M - \overline{X}_O}{\overline{X}_O}, \quad (3)$$

respectively, where $\overline{X}_M$ is the 20-year mean of NARCliM climate variables or the APSIM-simulated outputs forced by NARCliM climate and $\overline{X}_O$ is the 20-year mean of observed climate variables or the APSIM-simulated outputs forced by observations.

To ensure reliable analysis of the impact and/or the contribution of changes in climate variables or management practices, we need not only to assess the biases in climate variables, but also to remove biases in APSIM-simulated outputs associated with the climate biases. This bias correction of simulated outputs is termed as secondary bias correction (SBC; Yang *et al.*, 2016b) because it is applied after the "primary" bias correction of the climate model outputs. We used the method proposed by Haerter *et al.* (2011) that can correct both mean bias and bias in the variation of annual values as

$$Y = \overline{X}_{O,bl} + \frac{S_{O,bl}}{S_{M,bl}}\left(X_M - \overline{X}_{M,bl}\right), \quad (4)$$

where Y is the bias corrected value; X is APSIM-simulated outputs; the subscript O or M denotes, respectively, that driven by observed climate or RCM-simulated climate with bl for the baseline period 1990–2009; S is the standard deviation over the 20-year data and $\overline{X}$ is the 20-year mean. Hereafter, the data before SBC are denoted as NonSBC and after SBC as SBCMnSD. Although Equation (4) can reduce/correct some of the biases of the mean and interannual variation, it is obvious that the function is a linear that has been applied for correction of simulated crop yield resulted from a nonlinear process of biophysical models. Therefore, it is anticipated that such correction would work better for outputs resulted from less nonlinear processes or small magnitude of biases. In other words, further careful assessment or caution is needed for interpretation of the results involved in SBC.

In this study, the RCM bias is interchangeable with the term of climate bias as the bias in RCMs includes the bias inherited from GCMs.

3 | RESULTS

3.1 | RCM biases

The bias correction applied to the NARCliM data does not account for different biases in different seasons of the year. To examine residual biases for seasons relevant to cropping, we calculated biases of climate variables for each RCM simulation by comparing the NARCliM-simulated climate with the SILO observation within cropping periods (pre-sowing (PS); sowing to flowering (STF); flowering to harvesting [FTH]) as well as annually in the baseline period (1990–2009).

The distributions across the 370 study sites of MBEs in radiation, temperature and rainfall and their intra-standard deviation (intra-SD) of variations in daily sequences as well as rainfall probability and intensity for annual and three cropping periods (PS, STF and FTH) were shown in

Figures 2–4. Small annual-based biases in both magnitude and the variation across the 370 sites were found for all RCMs for all variables, except for radiation, for which biases were larger as this variable was not post-processing bias corrected due to radiation data unavailable in AWAP data set that were used for the post-processing bias correction of the NARCliM simulations (Figure 2). In addition, the annual-based biases in temperatures and rainfall probability were much small and consistent with RCMs, but that in intra-SD of temperature, rainfall and rain intensity were also quite large with systematically lower values compared to observations for all RCMs (Figures 3 and 4).

In the three cropping periods (PS, STF and FTH), almost all the RCMs over-estimated radiation (Figure 2a). Radiation MBEs exhibited an increased trend from PS to FTH. Biases for R3 simulations were larger than those for R1 and R2 simulations. However, the intra-SD of bias in radiation for FTH period had negative MBEs, largely positive before flowering (PS and STF) and annual (Figure 2b). As intra-SD measures the variability of daily sequences, a negative or positive intra-SD bias means the daily sequence of RCMs exhibits a larger or smaller daily variation than observed daily sequences, respectively. This indicates that the daily sequences of the NARCliM radiation were mismatched to the observations. It is worth noting, again, that the NARCliM radiation was not post-processing bias-corrected, and a large proportion of radiation in SILO was also calculated, rather than actually observed.

Unlike the consistent trending in radiation, the temperature MBE varied considerably between RCM simulations and crop growing periods (Figure 3). The most distinct feature was that the bias had a reciprocal low–high pattern between periods, that is, one higher value accompanied with another lower. For example, some RCM simulations (CC-, CS- and EC-RCM) produced higher minimum temperature (T_{min}) in PS period, but lower in another two phenological stages (STF and FTH) (Figure 3c). In comparison between temperature variables, RCMs gave a higher maximum temperature (T_{max}) in one period and often showed lower T_{min} for the same period. For example, CC-R1 had a median MBE of +0.7 °C for T_{max} in the period of FTH (Figure 3a), but −0.5 °C for T_{min} in that period (Figure 3c). The magnitude of MBEs was not the same for T_{min} and T_{max}, the MBEs for daily mean temperature (T_{mean}) were still large and maintained a similar pattern to T_{max} or T_{min}. Generally, more negative T_{mean} MBEs for STF period were found for CC-, CS- and EC-RCMs, but more positive T_{mean} MBEs were found by MI-RCMs for this important phenological period (Figure 3e). This may lead to biases in the phenological development as temperature is primary factor controlling crop phenology. Higher maximum temperatures may also lead to more events of extreme temperatures that can be extremely harmful for crops if they exceed certain values. The intra-SD MBEs for temperatures varied considerably, suggesting that the post-processing bias corrected NARCliM

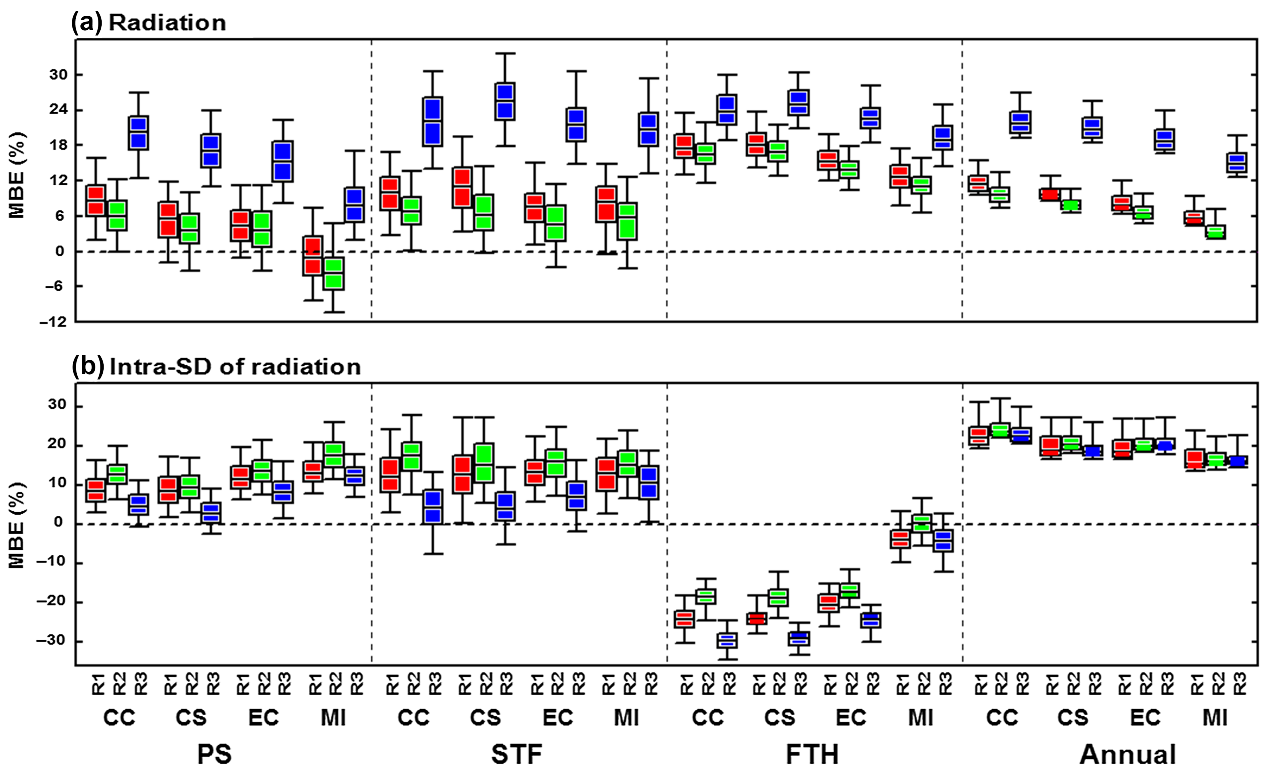

FIGURE 2 MBE in NARCliM-simulated radiation and intra-SD for the PS, STF, FTH and annually. The box plots show the 5, 25, 50, 75, and 95 percentiles, calculated from the 370 sites [Colour figure can be viewed at wileyonlinelibrary.com]

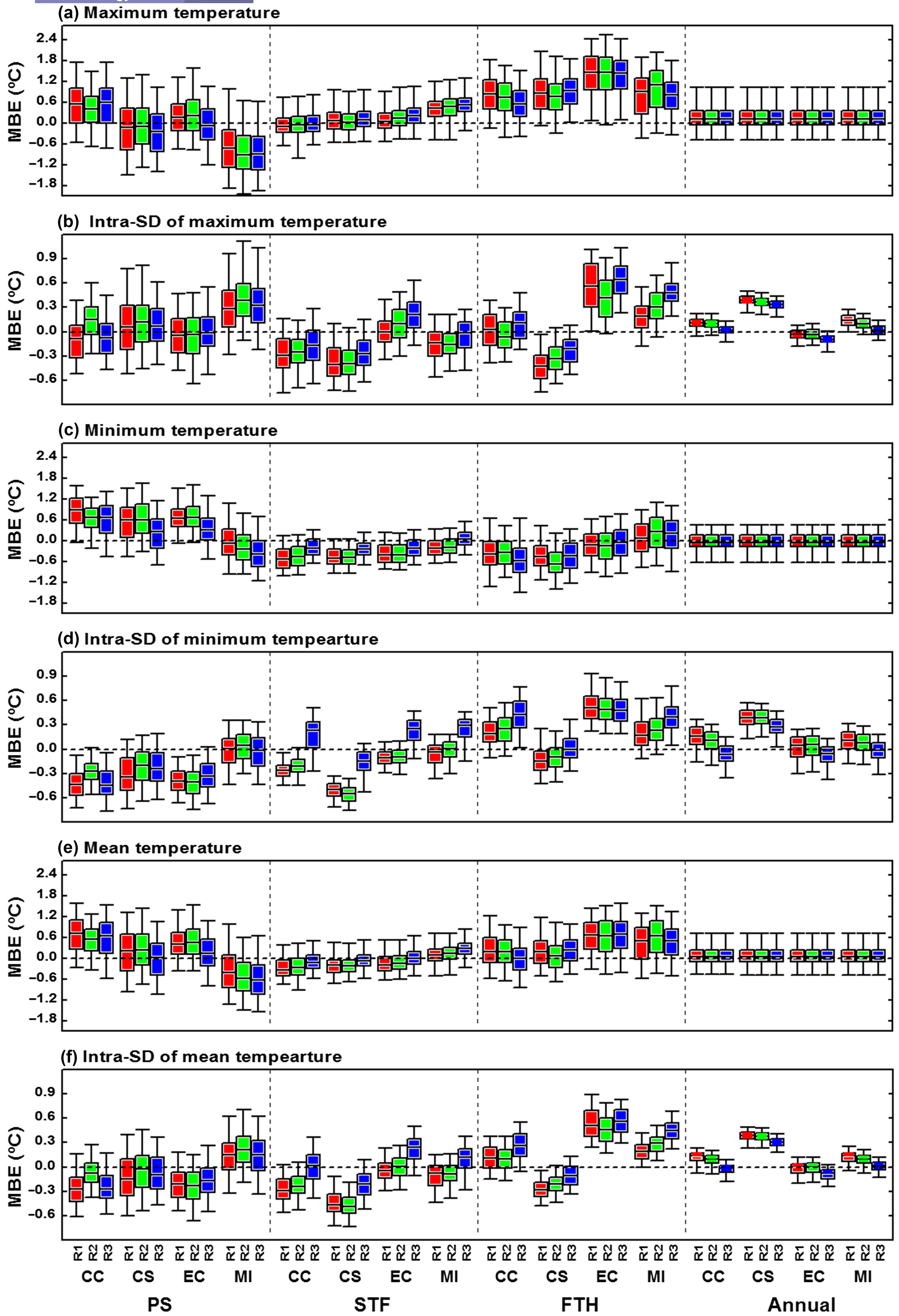

FIGURE 3 MBE in NARCliM-simulated maximum, minimum and mean temperatures and their intra-SD for the PS, STF, FTH and annually. The GCM-based R1, R2 and R3 are in red, green and blue colour, respectively. The box plots show the 5, 25, 50, 75 and 95 percentiles, calculated from the 370 sites [Colour figure can be viewed at wileyonlinelibrary.com]

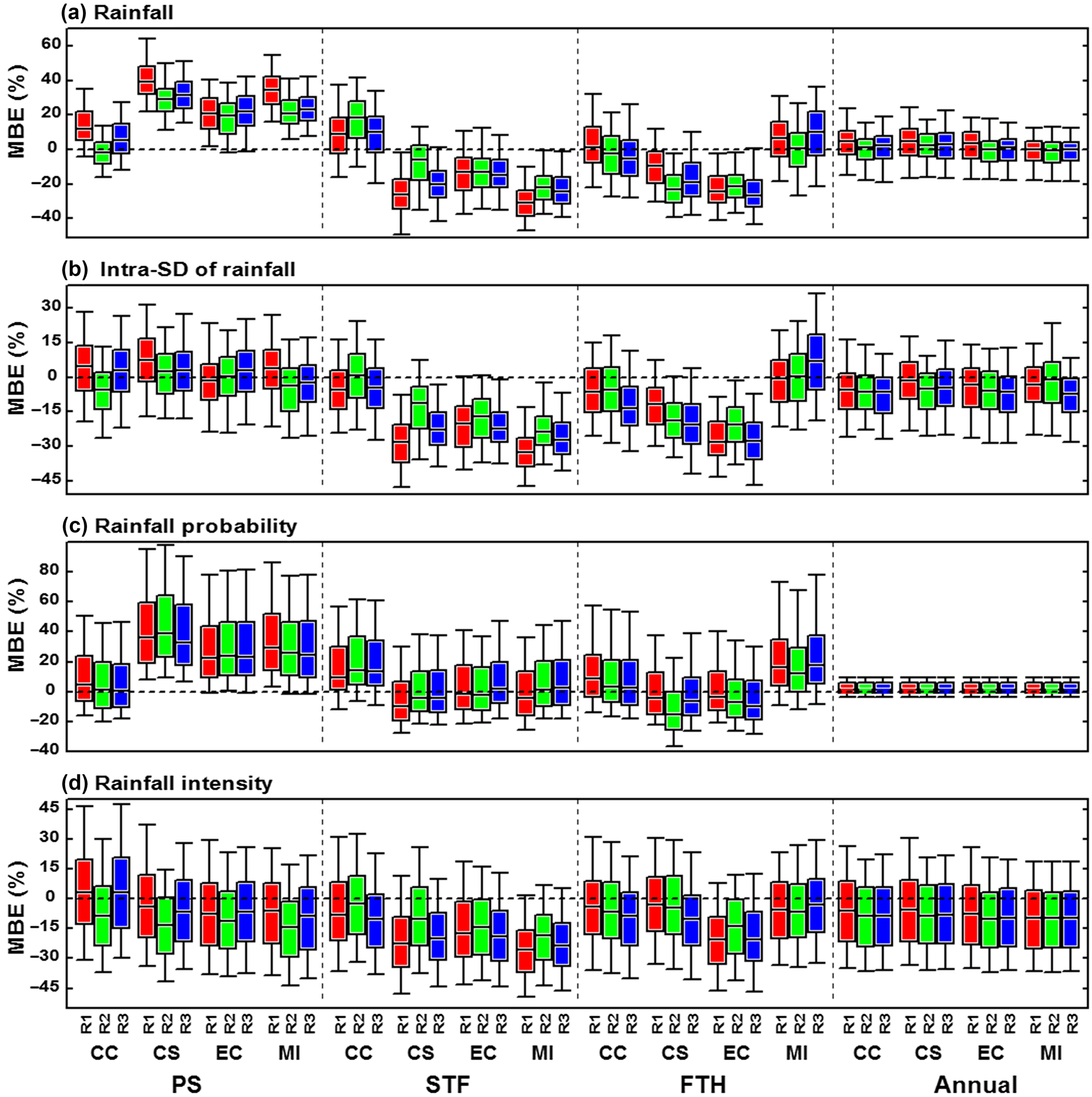

FIGURE 4 MBE in NARCliM-simulated rainfall and rainfall intra-SD, and MBE in rainfall probability and rainfall intensity for the PS, STF, FTH and annually. The box plots show the 5, 25, 50, 75 and 95 percentiles, calculated from the 370 sites [Colour figure can be viewed at wileyonlinelibrary.com]

data do not accurately reproduce the seasonal cycle in temperature (Figure 3b,d,f).

Rainfall biases also varied considerably across RCMs, which can be categorized in three distinct groups. First, the rainfall simulated by CC-RCMs had smaller range of biases for all periods than other RCMs, showing a narrow MBE interquartile from −10 to +30% (Figure 4a). Although the rainfall MBEs for the three CC-RCM simulations were still quite large, these RCMs showed better performance than these RCMs driven by other GCMs. The second group of RCMs (CS-RCMs and EC-RCMs) produced significantly higher rainfall in the PS period, but lower rainfall for the crop growing periods (STF and FTH), exhibiting a wide MBE interquartile from −40 to +50% across RCMs. The third group of RCMs (MI-RCMs) gave over 90% of sites with positive MBEs in PS period and negative MBEs in STF period. Generally, a similar seasonal bias pattern, that is, positive MBE in one period companied with a negative in another period, was found in rainfall bias, suggesting that the post-processing bias corrected NARCliM data do not accurately reproduce the seasonal cycle in rainfall. The intra-SD MBE for rainfall in the growing season was mostly negative, suggesting smaller variations in daily rain events than observations (Figure 4b).

In addition to analysis of rainfall MBE, we further explored the rain-event characteristics. Figure 4c,d exhibited an obvious contrasting pattern between rainfall probability (i.e., unconditional probability of a rain-day) and rainfall intensity, showing that the bias-corrected RCM outputs tended to produce a higher rainfall probability (Figure 4c) and lower rainfall intensity than observations (Figure 4d). This indicated that all RCMs simulated more frequent but less intensive rainfall when compared with SILO data.

Figure 5 shows the coherent relationship between three rainfall characteristics (intensity, probability and amount) MBEs because the three MBEs for each site are displayed together. For convenience, we arbitrarily considered the sites with all three rainfall characteristic MBEs are within the range from −10 to +10% as a *low bias* sites, showing in the shaded area (Figure 5). The results show several points worth noting. First, the performance of RCMs driven by different GCMs was different as CC-RCMs simulations exhibited 58–74% of sites with substantial wet biases (rainfall MBE ≥ +10%) (Figure 5a,c), but RCMs driven by other GCMs produced substantial dry bias (rainfall MBE ≤ −10%) for 77–95% of sites. The wet-bias RCMs (CC-RCMs) produced 11–18% sites with relative low bias, while none of the dry-bias RCMs (CS-, EC- and MI-RCMs) produced more than 10% of sites with low bias. Second, there was obviously a negative relationship between rainfall intensity MBE and probability MBE, that is, increasing in rainfall probability bias is associated with decreasing rainfall intensity bias. The relationship is largely well described by a linear relationship with a slope of −0.4 to −1.3 (% rainfall probability MBE per % intensity MBE) and intercept of −13.1 to −21.5 (% rainfall probability MBE) for negative rainfall sites, but +5.2 to +23.3 5 (% rainfall probability MBE) for positive rainfall bias. Third, the relatively small rainfall bias sites were deposed in a diagonal strip across the origin, while larger magnitudes of rainfall MBE had a parallel distribution above the low bias strip for positive or below for negative rainfall bias. These may suggest a systematic bias pattern related to the rainfall characteristics. Furthermore, the largest proportion of MBEs was distributed in the quadrant II (except for CS-R1 and CS-R2) representing these sites with positive rainfall probability MBE and negative intensity MBEs which were associated with either negative rainfall MBE for the dry-bias RCMs (i.e., CS-, EC- and MI-RCMs, Figure 5d,l) or positive rainfall MBE for the wet-bias RCMs (i.e., CC-RCMs) (Figure 5a,c). The second largest proportion of MBEs for the dry-bias RCMs was in the quadrant III where all sites had all negative MBEs for the three rainfall characteristics, comparing with the second largest proportion for the wet-bias RCMs (i.e., CC-RCMs) was in quadrant I with all positive MBEs for the three rainfall characteristics. The results indicated that RCMs tended to simulate smaller, but more frequent rain-events whether with smaller or larger amount of rainfall in the crop growing period, or smaller amount of rainfall associated with lower intensity or fewer rain-events than observations for most sites in the MRC region. It is clear that either type of rainfall can reduce or alter the availability of soil water for crop growth and downstream water in rivers, hence, likely produce different biophysical modelling outputs.

In addition, linear regression analysis on all data for each RCM showed that the 89–93% rainfall probability MBE variance was accounted for by the intensity MBE and growing season rainfall MBE with their respective slopes ranged from −1.1 to −1.3 and +0.9 to +1.1. We further summarized the relationships of the rainfall characteristic MBEs over the study area, that is, with the 370 sites, by the following relationship:

$$\mathrm{MBE}_i = 0.06^{**} - 0.65^{***}\mathrm{MBE}_f + 0.72^{***}\mathrm{MBE}_p,\ R^2 = 0.96, \tag{5}$$

where subscripts, *i*, *f*, *p* denoted rainfall intensity, rainfall probability and growing season rainfall, respectively.

3.2 | Biases in APSIM-simulated parameters

3.2.1 | Biases in APSIM-simulated soil water and N uses under farming management

We compared the biases in a wide range of APSIM-simulated outputs through the difference between the outputs forced by RCMs and those forced by observed climate (SILO). Biases in APSIM-simulated soil water balance, crop phenology and production are shown in Figures 6–8. Figure 6a shows that more RCMs resulted in positive MBE in soil water at sowing (SWS). However, the biases in runoff (RO) (Figure 6b) and deep drainage (DD) (Figure 6c) were negative at the majority of sites, except for DD for the three CC-RCM simulations. The biases in soil water evaporation (ES) were positive at almost all sites (Figure 6d). It is noticeable that ES biases associating with R3 were consistent higher than R1 or R2 (Figure 6d), reflecting the higher radiation (Figure 2a) that was inputted into the biophysical model and driven the energy-based soil evaporation processing.

In addition, across around 75% of 370 sites, biases in plant transpiration (EP) were positive when APSIM simulation were forced by the three CC-RCMs and negative for the rest of nine RCMs (Figure 8a). These results were highly correlated with the biases in the rainfall simulations. For example, CC-RCMs that produced positive EP are the RCMs that had positive rainfall biases, while the RCMs driven by other GCMs resulted in negative EP MBE largely due to their negative rainfall biases. Moreover, because plant N uptake follows water uptake, the biases in APSIM-simulated N-uses (NU) exhibited a similar pattern to EP biases (Figure 8b).

Importantly, there was a clear interaction between the biases and farming management practice. For example, the crop residue incorporation (RI) considerably reduced the range of the SWS bias, DD bias and plant transpiration bias at RI0 (Figures 6a,c and 8a), but increased the magnitude of the negative RO MBE in RI100. Similarly, a larger

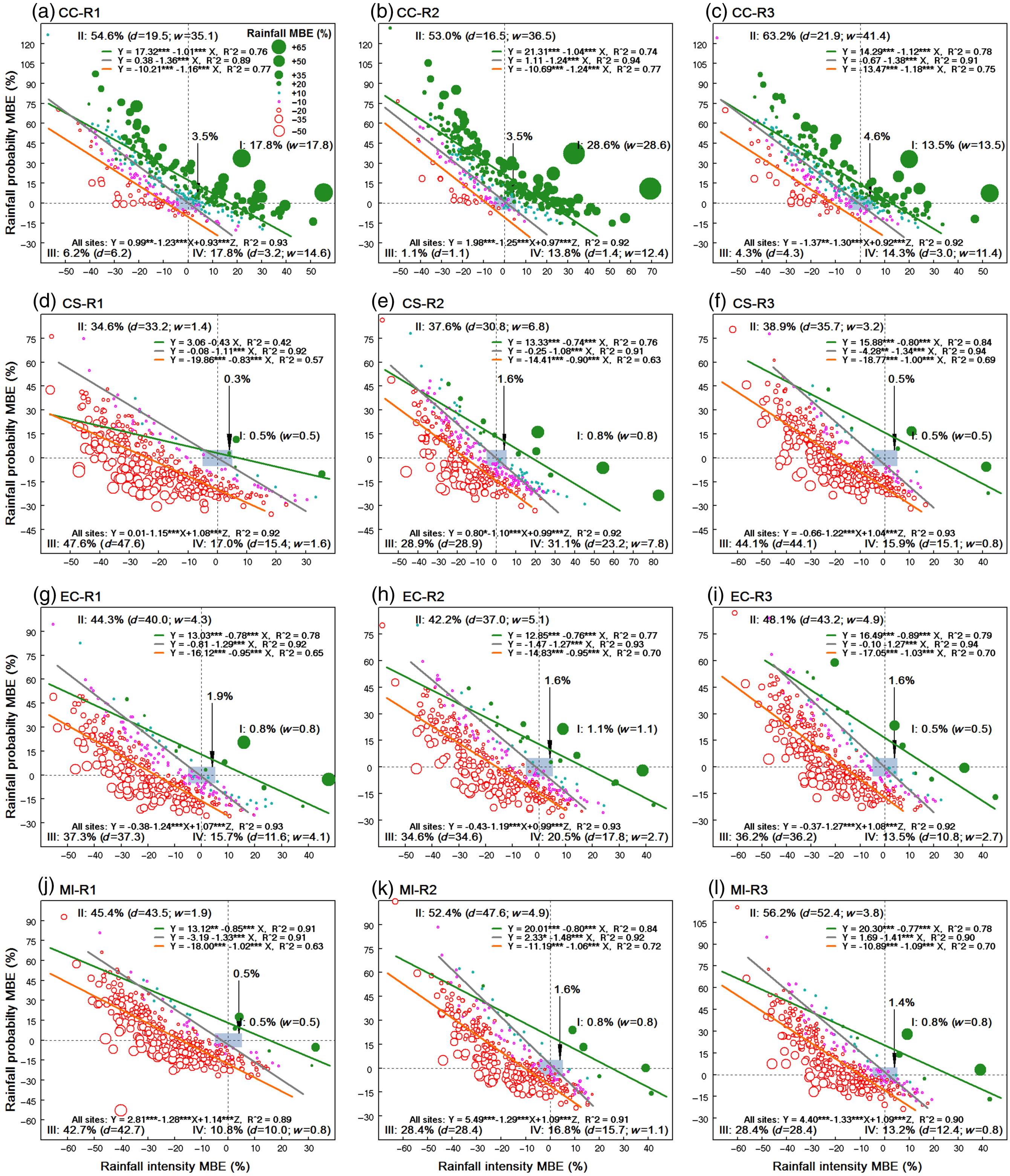

FIGURE 5 Relationship between rainfall intensity MBE, rainfall probability MBE and the amount MBE in crop growth period for the 370 sites in MRC region of New South Wales, Australia. Grey shading represents where MBEs in all rainfall variables are less than 10% and the proportions of sites falling within these areas are noted at the end of the black arrows. The proportion of sites with MBE greater than 10% for one or more rainfall variables is shown for each quadrant, followed by the proportion showing dry bias (*d*) and/or wet bias (*w*) in the brackets. Linear least squared regression was applied to the sites with the rainfall MBE ≤ −10%, −10 to <+10% and ≥+10%. All data were fitted to the rainfall probability MBE (*Y*, %) as a linear function of rainfall intensity MBE (*X*, %) and the amount of rainfall MBE (*Z*, %). The coefficients with *, ** and *** are significant at $p < .05$, $p < .01$ and $p < .001$, respectively, otherwise, not significant [Colour figure can be viewed at wileyonlinelibrary.com]

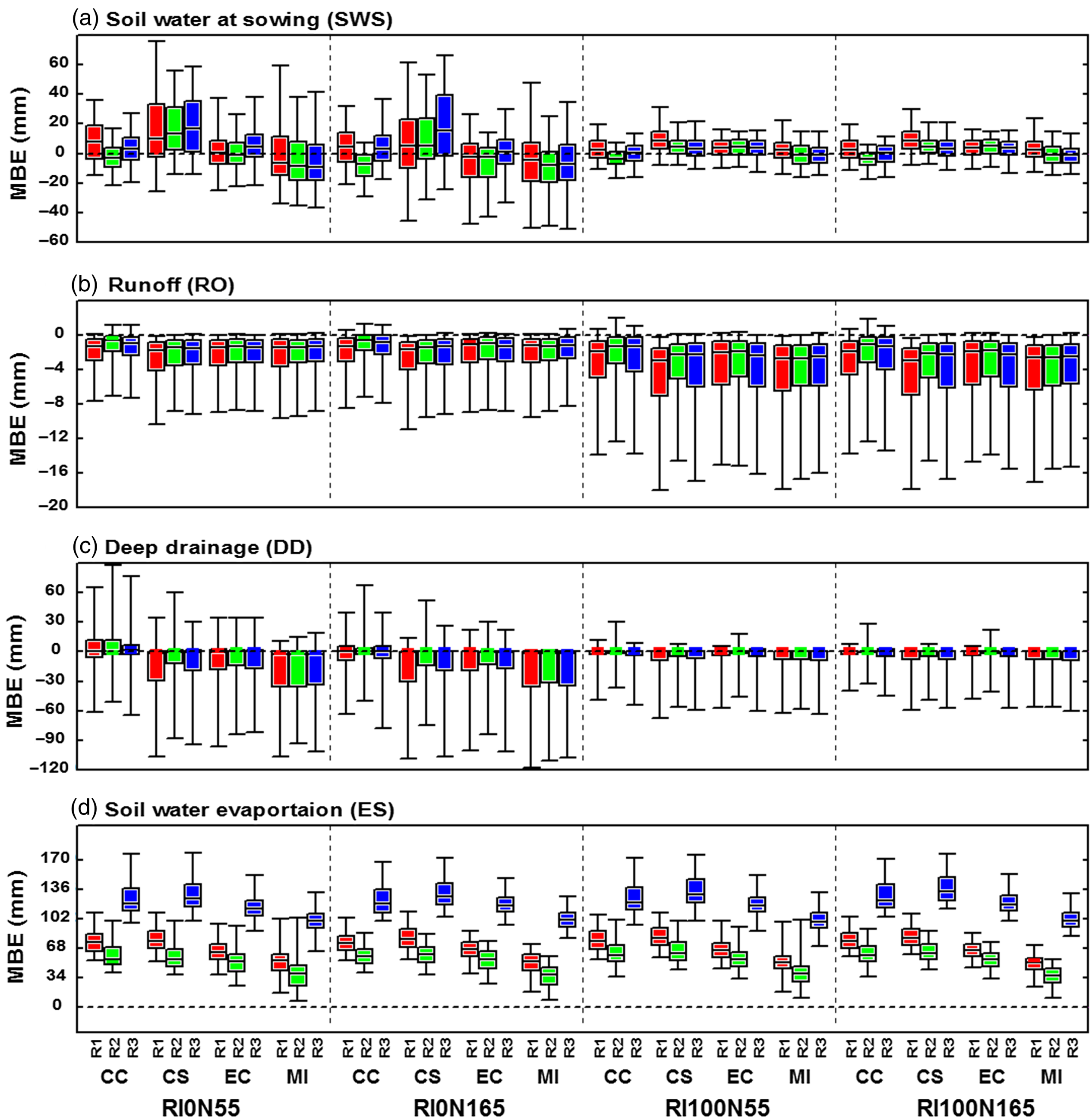

FIGURE 6 MBE in APSIM-simulated soil water balance outputs under the four management treatments (RI0N55: 0% residue incorporation by 55 kgN/ha; RI0N165: 0% residue incorporation by 165 kgN/ha; RI100N55: 100% residue incorporation by 55 kgN/ha; RI100N165: 100% residue incorporation by 165 kgN/ha). The box plots show the 5, 25, 50, 75 and 95 percentiles, calculated from the 370 sites [Colour figure can be viewed at wileyonlinelibrary.com]

magnitude of biases in EP and NU were simulated at a high N-application than lower N-application (Figure 8a,b). The study reveals that farm management practice may interact with the climate biases and consequently affect biases in biophysical modelled outputs.

3.2.2 | Biases in APSIM-simulated plant development and crop growth

For MI-RCMs, approximately 75% of sites had a SD later than that resulting from observed climate, while the RCMs driven by other GCMs exhibited more negative SD biases (Figure 7a). The number of days from STF and crop duration (CD) simulated by APSIM forced by CC-, CS- and EC-RCMs were generally longer (positive MBE) at most sites and those forced by MI-RCMs were shorter (negative MBE), relative to APSIM simulations forced by observed climate (Figure 7b,c). It is not surprising that the differences in crop phenological biases were consistent with the biases in NARCliM projected temperature, that is, the MI-RCMs that produced a faster development (negative positive DTF and CD MBE) (Figure 7b,d) in crop development were the RCMs that had positive T_{mean} biases in this phenological period (Figure 3e).

Similarly, the three CC-RCMs showed positive biomass bias in over 75% sites, largely resulted from the

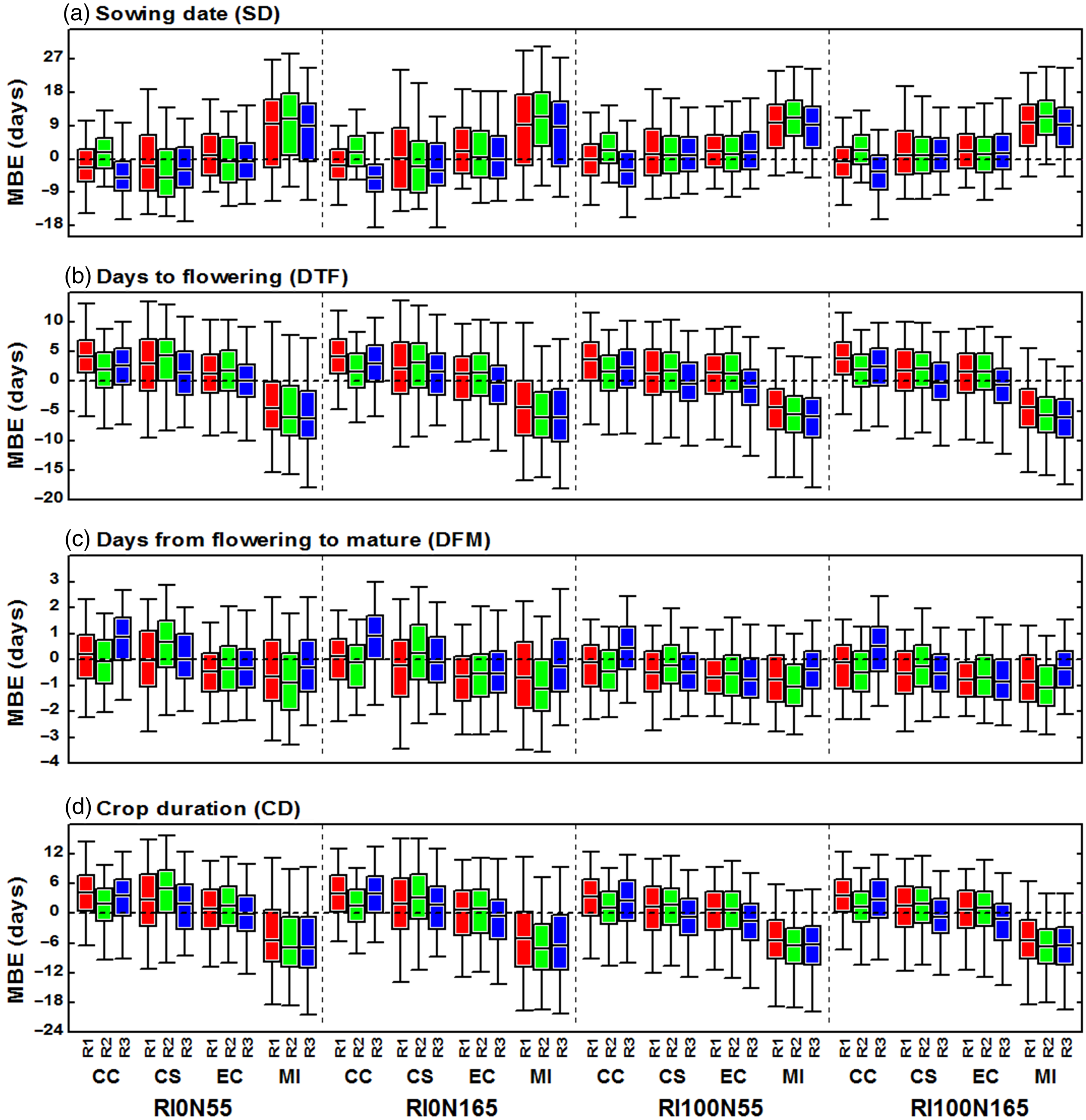

FIGURE 7 MBE in APSIM-simulated wheat phenology outputs under the four management treatments (RI0N55: 0% residue incorporation by 55 kgN/ha; RI0N165: 0% residue incorporation by 165 kgN/ha; RI100N55: 100% residue incorporation by 55 kgN/ha; RI100N165: 100% residue incorporation by 165 kgN/ha). The box plots show the 5, 25, 50, 75 and 95 percentiles, calculated from the 370 sites [Colour figure can be viewed at wileyonlinelibrary.com]

positive rainfall MBEs. However, the large positive biomass biases by CC-RCMs (Figure 8c) are not apparent for wheat yield (Figure 8d), due to the difference in the rainfall biases from the positive rainfall biases in STF period to a negative rainfall biases in FTH period produced by these RCMs (Figure 4a). This is also because wheat biomass gain largely occurs before pre-flowering. The nine RCMs driven by CS, EC and MI exhibited negative biases in both wheat biomass and wheat yield in most sites, corresponding to the same pattern of the biases in rainfall and ultimately plant transpiration (Figures 4a and 8a). In addition, for these dry RCM simulations (CS-, EC- and MI-RCMs), the high rate of N application with residue removal produced the largest interquartile range for both wheat biomass and yield biases, but that with the 100% RI gave a relative small range (Figure 8c,d), suggesting that the relative importance of climate biases in APSIM outputs can change with the simulated management.

3.3 | Spatial distribution of wheat yield biases affected by farm management practice

In the baseline period (1990–2009), APSIM-simulated wheat yield with observed weather data in the four treatments (RI0N55, RI0N165, RI100N55 and RI100N165) increased

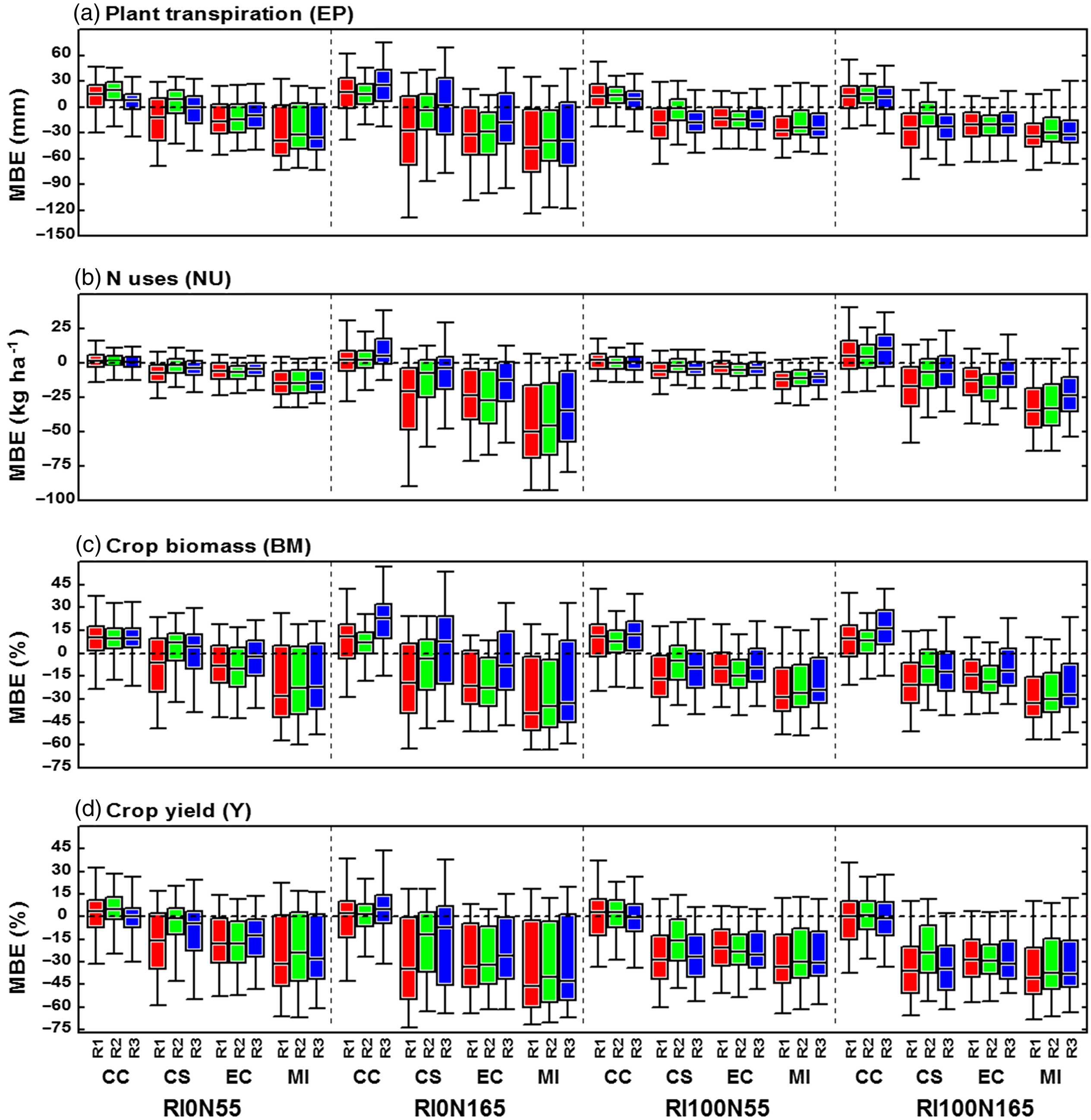

FIGURE 8 MBE in APSIM-simulated outputs of plant transpiration (a), N uses (b), wheat biomass (c) and wheat yield (d) under the four management treatments (RI0N55: 0% residue incorporation by 55 kgN/ha; RI0N165: 0% residue incorporation by 165 kgN/ha; RI100N55: 100% residue incorporation by 55 kgN/ha; RI100N165: 100% residue incorporation by 165 kgN/ha). The box plots show the 5, 25, 50, 75 and 95 percentiles, calculated from the 370 sites [Colour figure can be viewed at wileyonlinelibrary.com]

from west to east, corresponding to rainfall gradient from low to high (Figure 9). The average yield ranged from 2.6 t/ha for RI0N55 to 3.7 t/ha for RI0N165, closely representing the recent wheat yield in this region (Wang *et al.*, 2015).

The spatial distribution of the APSIM-simulated yield MBEs exhibited a number of distinct patterns related to different RCMs and farming managements. First, there were large variations between RCMs driven by different GCMs. The smallest yield MBEs were found in the three CC-RCMs and largest yield MBEs were observed in MI-RCMs driven wheat yields. Taking RI0N55 for example, the magnitudes of wheat yield MBE showed an increased order of CC-, CS-, EC- and MI-RCMs with the range of mean yield MBEs of −0.6 to 2.2%, −16.5 to −4.8%, −17.4 to −14% and −24.1 to −21.6%, respectively (Figure 10). Second, MBEs had a clear spatial pattern from relatively large negative MBE in the west region to relatively large positive MBE in the east region. Third, the magnitude of yield MBE in the high N treatment was larger than in the low-N treatment because negative bias in soil water can restrict up-take of abundant nitrogen (high N applied) available in the soils and because in the low N treatment, N availability is much more restricting and governing than water availability and water variation (from rainfall), hence increasing the consequence of rainfall

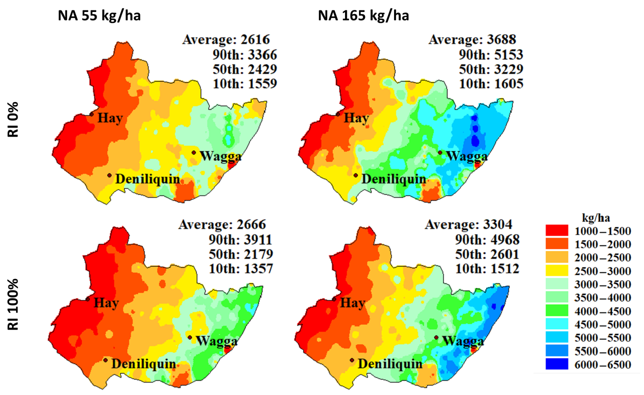

FIGURE 9 Historical mean annual wheat yields simulated by APSIM forced by SILO observed climate data under the four management treatments (0% residue incorporation by 55 kgN/ha; 0% residue incorporation by 165 kgN/ha; 100% residue incorporation by 55 kgN/ha; 100% residue incorporation by 165 kgN/ha) [Colour figure can be viewed at wileyonlinelibrary.com]

biases on crop growth, again, suggesting that farm management practice can interact with climate biases, hence enlarge the wheat yield biases.

3.4 | Relationships between the RCMs biases and the responding biases in biophysical modelled outputs

The relationships between the biases in NARCliM-simulated climate and the biases in APSIM-simulated variables were established by the analysis of least squared multiple regression (Table 2). Prior to the regression analysis, we calculated the variance inflation factor (VIF; Doetterl *et al.*, 2015) to detect whether there is any statistical evidence of collinearity among climate MBEs (i.e., MBE_R, MBE_T and MBE_P for MBE in radiation, temperature and rainfall, respectively) in each of 370 sites. VIF is defined as the reciprocal of $1 - R^2$, that is, $VIP_i = 1/\left(1-R_i^2\right)$ (Stine, 1995), hence VIF varies from 1 to $+\infty$. The R_i^2 is the coefficient of determination from the regression of the *i*th variable on the other variables. If the *i*th variable cannot be explained by other variables at all, that is, $R_i^2=0$, $VIP_i = 1$. If the *i*th variable can be completely explained by other variables, that is, $R_i^2 \rightarrow 1$, $VIP_i \rightarrow +\infty$. The results showed that the highest VIF was 5.7 and the overall mean VIF was 1.4 across 370 sites, indicating that these climate MBEs do not exhibit significant collinearity as none of them was greater than the threshold (10) for significant collinearity (Doetterl *et al.*, 2015) (data not shown).

The regression coefficients quantified the contributions of the RCM biases to the biases in the biophysical modelled outputs. The overall mean values of the coefficients and their regression statistics (R^2 and the standard error (*SE*) of estimate) are also shown in Table 3. Generally, different MBE of climate variables had different effects on the MBE in the APSIM-simulated outputs due to the different functionalities of climate variables implemented in the crop model. For example, the biases in crop phenology (MBE_{DTF}, MBE_{FTH} and MBE_{CD}) were significantly correlated with T_{mean} MBE for 95–97% of 370 sites which contrasts to 24–66% of 370 sites for radiation and rainfall MBEs (Table 3). As temperature is the primary factor driving crop phenology in APSIM through cumulative thermal time, the resultant crop phenology MBE from temperature MBE is not unexpected. The results showed that per Celsius degree of T_{mean} MBE led to wheat flowering moving forward by 15 days (−15 days of bias) (Table 2) which is similar to the results of climate change impact as reported by Anwar *et al.* (2015) who found wheat flowering date advanced by 9–20 days per Celsius degree increase in future temperature. Moreover, the bias in SWS and SD were highly correlated with the biases in PS temperature and rainfall (Table 2). However, biases in DD and NU exhibited weak relationships to RCMs MBEs (lower R^2 of 0.44 and 0.50, respectively), because they did not directly link to the climate inputs. Generally, for variables influencing complicated physical or biological processes such as plant transpiration or crop growth, the biases in APSIM-simulated outputs were highly related to all biases of RCM-simulated variables (i.e., radiation, temperature and rainfall), indicated by 56–87% significant coefficients revealed for these variable (Table 2). The results confirmed that the biases in climate variables impacted upon the biases in APSIM-simulated outputs through the functionalities of these climate variables in the biophysical model.

3.5 | Effect of secondary bias correction on the impact of climate change on wheat yield

The distributions of RCM-driven NonSBC and SBCMnSD yearly wheat yields for 1990–2009 of the 370 sites with four management options are shown in Figure 11. Observation-driven yields had two peaks of 0.6 and 5.8 t/ha, which represented the western low-yield sites and the eastern high-yield sites, respectively (Figure 9). The distribution of CC-RCMs driven wheat yield was relatively close to that of observation-driven wheat yield, reflecting lower climate MBE. The yield distributions of CS-RCMs, EC-RCMs and MI-RCMs largely skewed low, hence forming much higher density at the low-yield peak and much lower density at high-yield peak than the observed PDF (Figure 11a). Applying the SBC resulted in yield distribution similar to observation-driven yield PDF (Figure 11b). Similar results will be reported for other crops including canola and lupin in the same region and the same RCM simulations elsewhere (Wang *et al.*, unpublished).

We calculated the yield changes based on the average of the 20-year yearly values. With the combination of 12 RCM simulations, four treatments and two future periods for each site, we quantified the effects of changes in climate variables, elevated CO_2 concentrations and crop management practice (RI and NU) on crop yield using a multiple linear regression (see the caption of Figure 12 for the equation).

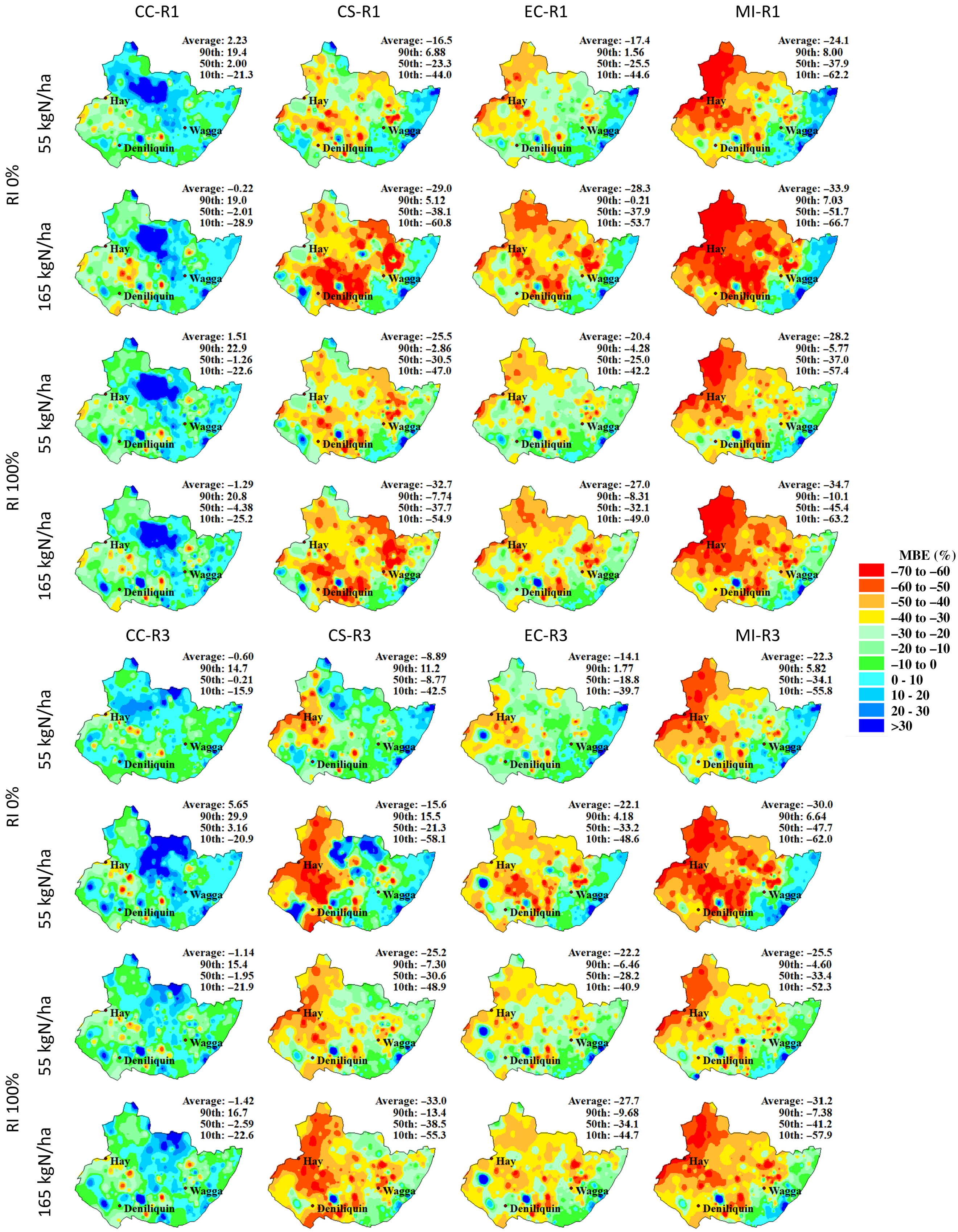

FIGURE 10 Spatial distribution of MBE in mean annual wheat yields simulated by APSIM forced by NARCliM simulations (four GCMs downscaled by R1 and R3 RCMs) for the combined treatments of 0% residue incorporation and 100% residue incorporation with N-application of 55 and 165 kg/ha [Colour figure can be viewed at wileyonlinelibrary.com]

TABLE 2 The coefficients and statistics of the multiple linear least squared regression of biases in APSIM-simulated parameters as a function of radiation MBE (MBE_R, %), temperature MBE (MBE_{Tmn}, °C) and rainfall MBE (MBE_P, %) in the formula of $MBE_{APSIM} = a\ MBE_R + b\ MBE_{Tmn} + c\ MBE_P$, where MBE_{APSIM} are biases in APSIM-simulated parameters (e.g., SWS, RO, DD, ES, EP, NU, SD, DTF, FTH, CD, BM = biomass; Y = yield). The mean coefficient and the standard deviation (±*SD*) are shown, followed by the percentage of sites with significant coefficient ($p < .05$) in brackets, where more than two thirds of 370 sites (≥67%) with a significant coefficient are in bold. *SE* is the standard error of the estimate

APSIM variables	Period[a]	*a* $\%^{-1}$	*b* $°C^{-1}$	*c* $\%^{-1}$	R^2	*SE*
MBE_{SWS} (days)	PS	0.05 ± 0.33 (25)	10.00 ± 7.29 (**79**)	0.17 ± 0.36 (65)	0.60 ± 0.20	9.76 ± 4.70
MBE_{SD} (days)	PS	−0.09 ± 0.19 (51)	−8.06 ± 3.43 (**94**)	0.12 ± 0.16 (**80**)	0.80 ± 0.18	3.74 ± 1.78
MBE_{RO} (mm)	GS	−0.09 ± 0.09 (**84**)	−0.03 ± 6.02 (45)	0.11 ± 0.18 (**83**)	0.72 ± 0.18	1.74 ±1.87
MBE_{DD} (mm)	GS	−0.12 ± 0.35 (33)	−2.90 ± 31.90 (29)	0.84 ± 1.33 (55)	0.44 ± 0.26	11.03 ± 11.89
MBE_{ES} (mm)	GS	−0.01 ± 0.38 (34)	−21.86 ± 17.31 (**75**)	0.53 ± 0.30 (**82**)	0.64 ± 0.14	11.75 ± 5.51
MBE_{EP} (mm)	GS	0.05 ± 0.66 (59)	−35.26 ± 28.52 (**78**)	0.84 ± 0.70 (85)	0.73 ± 0.19	15.35 ± 6.57
MBE_{NU} (kg)	GS	0.66 ± 0.67 (66)	21.97 ± 31.56 (46)	−0.16 ± 0.46 (27)	0.50 ± 0.19	19.84 ± 8.38
MBE_{DTF} (days)	STF	−0.01 ± 0.11 (52)	−15.19 ± 7.30 (**95**)	0.06 ± 0.07 (66)	0.80 ± 0.17	2.35 ± 1.10
MBE_{FTH} (days)	FTH	0.01 ± 0.04 (58)	−1.72 ± 0.78 (**97**)	0.00 ± 0.01 (24)	0.86 ±0.17	0.40 ± 0.30
MBE_{CD} (days)	GS	0.02 ± 0.12 (58)	−16.91 ± 7.18 (**97**)	0.04 ± 0.08 (39)	0.87 ± 0.16	2.12 ± 1.35
MBE_{BM} (%)	GS	0.14 ± 0.56 (**70**)	−25.40 ± 17.11 (**83**)	0.61 ± 0.54 (**86**)	0.76 ± 0.15	10.12 ± 3.28
MBE_Y (%)	GS	−0.46 ± 0.61 (56)	−15.12 ± 17.14 (57)	0.74 ± 0.64 (**87**)	0.72 ± 0.26	10.99 ± 3.57

[a] Bias period: the period of NARCliM MBE used for the regression. FTH = flowering to harvesting; GS = growing season (sowing to harvesting); PS = pre-sowing (February 1 to sowing date); STF = sowing to flowering.

TABLE 3 VIF and the collinearity for the changes in climate (radiation: Δ*R*; temperature: Δ*T*; rainfall: Δ*P*; [CO_2]: ΔCO_2) and management variables (crop residue incorporation: ΔRI; N-uses: ΔNU). Data without SBC (NonSBC) and with SBC (SBCMnSD) are analysed for the comparison. The rate of collinearity (ColR, %) is shown for individual change factor or on-site based when one or more change variable is collinearity

Percentile		Δ*R*	Δ*T*	Δ*P*	ΔRI	ΔNU	ΔCO_2	Site ColR (%)
Wheat								
NonSBC	M_{VIF} ± *SD*	7.0 ± 3.5	10.8 ± 4.5	3.1 ± 2.7	2.1 ± 0.4	2.7 ± 0.6	16.3 ± 5.6	
	ColR (%)	10.5	48.1	0.3	0.0	0.0	94.9	95.1
SBCMnSD	M_{VIF} ± *SD*	4.5 ± 1.5	4.1 ± 1.8	3.21 ± 0.88	2.1 ± 0.5	2.5 ± 0.6	6.1 ± 2.1	
	ColR (%)	0.5	1.1	0.0	0.0	0.0	4.3	4.9

With this regression analysis, the contribution of specific climate factors to yield change can be quantified. Here we used climate change and the yield change with and without SBC (i.e., the data of SBCMnSD and NonSBC) to differentiate the effectiveness of SBC. Figure 12 shows the wheat yield change could be well described by the changes in radiation (Δ*R*), mean temperature (ΔT_{mn}), rainfall (Δ*P*) and CO_2 (ΔCO_2), and management practices, that is, incorporated

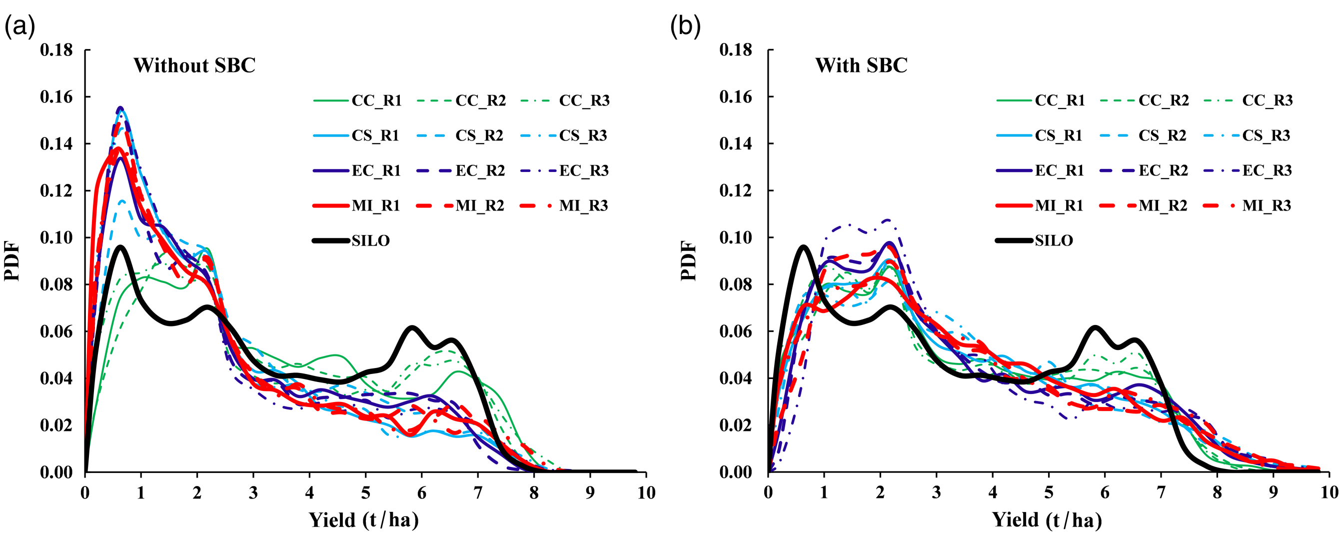

FIGURE 11 Probability distributions of baseline annual wheat yield simulated by APSIM forced by 12 NARCliM simulations and SILO observed climate data for data without SBC (NonSBC) and with SBC (SBCMnSD) [Colour figure can be viewed at wileyonlinelibrary.com]

crop residue (ΔRI) and NU (ΔNU), resulting in averaged R^2 of 0.83 for NonSBC outputs and 0.85 for SBCMnSD outputs and <10% for *SE* of estimate in most of cases. Although the absolute values of R^2 did not differ greatly between NonSBC and SBCMnSD, the benefits of the SBCMnSD are significant as explained below. It was evident that regardless of using data with SBC or without SBC, the change in wheat yield was negatively correlated to the change of future growing season radiation but positively correlated to changes in rainfall, NU and more residue incorporation (Figure 12). For the remaining variables (temperature and CO_2), the slopes of regressions were inconsistent both in terms of magnitudes or change direction, depending on locations or the data with or without SBC. There are two distinct differences between the NonSBC and SBCMnSD results. First, some coefficients derived from NonSBC outputs were meaningless. For example, the median of the coefficients quantifying CO_2 response by NonSBC yields were −2.4% [100 ppm CO_2]$^{-1}$ for wheat which contradicts the general understanding of CO_2 fertilization. After applying SBC, the median became +3.5% [100 ppm CO_2]$^{-1}$, which resulted in a CO_2 fertilization rate of 13.3% yield increase for doubling the current [CO_2]. Although this rate was still less than a rate measured through an experimental approach reported by Pandey *et al.* (2017), SBCMnSD outputs exhibited positive CO_2 coefficients across almost the entire region, instead of largely negative CO_2 coefficients with NonSBC outputs. Second, the coefficients associated with NonSBC yields varied dramatically, while those with SBCMnSD were much more consistent and closer to those previously reported. For example, the coefficients for temperature change by NonSBC showed a 10th–90th percentile range from −1.4 to 23.2%/°C for wheat, compared with the range from −6.5 to 4.8%/ C after bias correction (SBCMnSD). The results from SBC were consistent with previous reported temperature effects on future wheat (i.e., Wang *et al.*, 2017). In contrast, the average coefficients measuring the effect of ΔRI if the yields were not subjected to bias correction were consistently lower than those after SBC. For instance, 5.5%/tRI resulting from NonSBC yields for wheat was lower than 7.9%/tRI obtained from SBCMnSD yields, compared to 6.2–8.7%/tRI reported by Liu *et al.* (2017). One of the possible reasons to explain

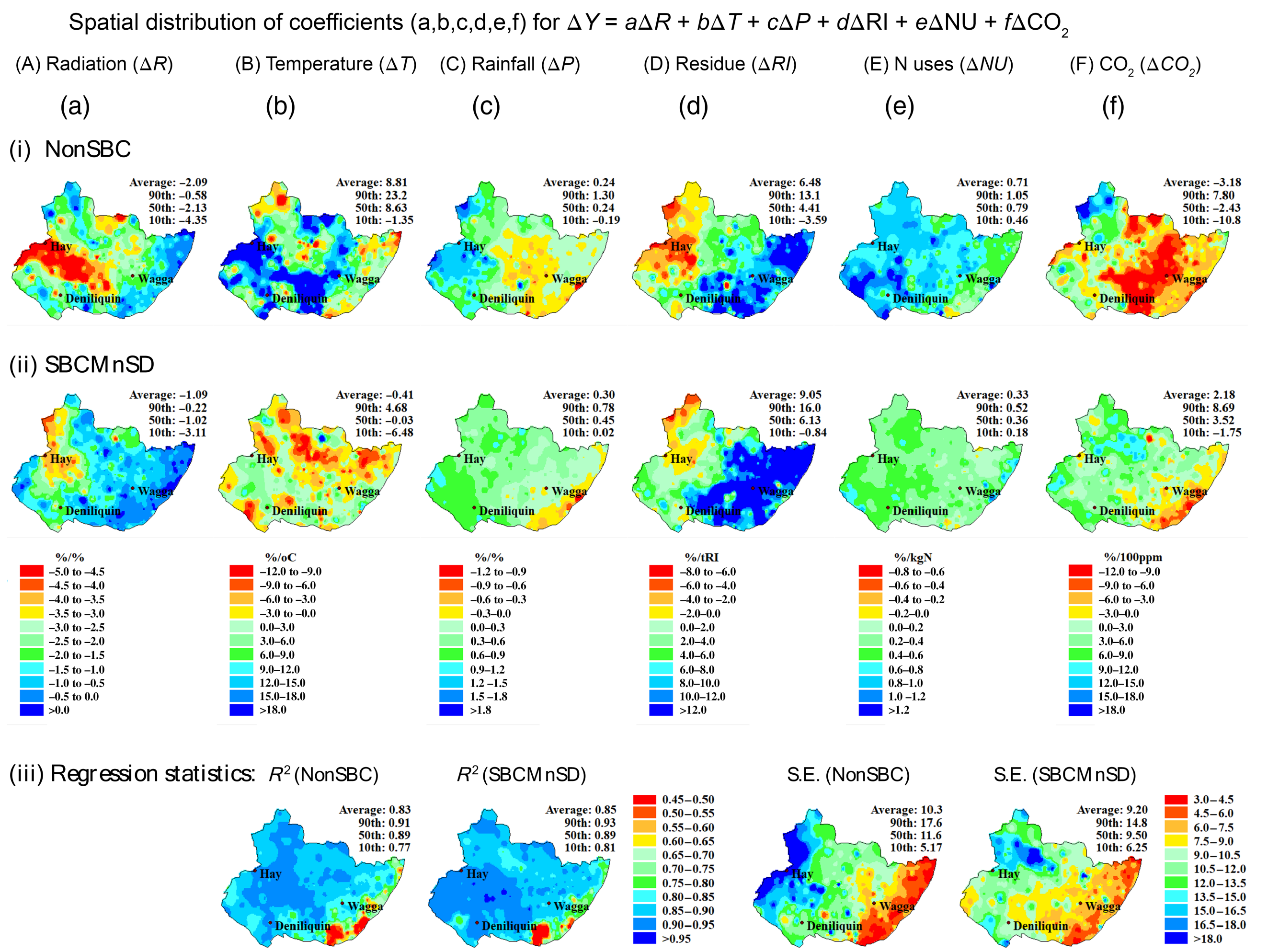

FIGURE 12 Spatial distribution of the coefficients of multiple least squared regression of wheat yield change (ΔY, %) as a function of changes in climate (radiation: ΔR, %; temperature: ΔT, °C; rainfall: ΔP, %; [CO_2]: ΔCO_2, 100 ppm) and management (crop residue incorporation: ΔRI, t/ha; N-uses: ΔNU, kgN/ha) in the formula, for data without SBC (NonSBC) and with SBC (SBCMnSD). Also included are the coefficient of determination (R^2) and *SE* of the regression analyses [Colour figure can be viewed at wileyonlinelibrary.com]

the different RI rate between NonSBC and SBCMnSD is the reduction of the effectiveness of residual incorporation due to the negative rainfall bias because water is the media for residual decomposition. The results indicated the biases in climate variables can result in confounding contributions to biophysical modelled outputs and increased uncertainties with effects of climate change and farm management practice.

In addition, SBC can effectively reduce the collinearity of climate and management variables. The results show that without SBC, ΔCO_2 exhibits strong collinearity with other variables, resulting in 95% of sites with VIF ≥ 10 for wheat (Table 2), compared to the 4% for SBCMnSD. Similarly, the next highly collinear variable was temperature that had 48% of sites showing VIF ≥ 10 with the data of NonSBC variables, but 1% of sites with the data of SBCMnSD variables. It is interesting to note that all management options (management practise) (ΔRI and ΔNU) and change in rainfall (ΔP) did not exhibit collinearity, regardless of data with or without SBC. Overall, 95% of sites had at least one variable showing collinearity if the biases in these variables were not corrected. But less than 5% of sites had collinearity when the SBC was applied. Therefore, the coefficients resulting from SBCMnSD significantly could provide a reliable estimate of the effect of climate change and management impacts as the SBC reduced the uncertainties in NonSBC outputs that were the attributors for collinearity.

4 | DISCUSSION

Dynamical downscaling consistently improves the spatial details of simulated climate compared to GCMs (Di Luca *et al.*, 2016). However, RCMs can inherit systemic biases from GCMs and also can generate additional uncertainties in their downscaling procedures (Giorgi *et al.*, 2001). Approaches to improve RCMs outputs are either by eliminating the effects of GCMs biases by driving RCMs with initial and boundary inputs of bias-corrected GCM data or by removing the biases from RCM simulations with post-processing bias correction. A number of reports (Jin *et al.*, 2011; Xu and Yang, 2012) demonstrated that dynamically downscaled outputs forced by bias-corrected GCM data as inputs resulted in significantly improved RCM outputs. Similarly, post-processing bias correction was also demonstrated as an effective approach in removing the biases in the outputs of RCM simulations (Di Luca *et al.*, 2018). The NARCliM project adopted the post-processing bias correction approach and studies have demonstrated some success in correcting biases in extreme rainfall and other rainfall characteristics (Argüeso *et al.*, 2013; Evans *et al.*, 2017). Our analysis showed that the data contained small magnitude biases in rainfall and temperature on an annual basis, but much larger magnitude of biases within cropping periods. This suggests that post-processing bias correction insufficiently corrected the seasonal biases, which is in agreement with Manage *et al.* (2016) who showed the seasonal cycle in the NARCliM data was stronger than seasonal cycle present in observed climate. Our study suggested that further investigations into bias correction should focus on removing the seasonal biases by undertaking bias correction at finer temporal scales such as seasonal or monthly.

In the cropping periods, NARCliM simulations exhibited substantial biases in temperature and rainfall which varied from RCMs driven by different GCMs and sites. The warm or cold temperature biases can lead to faster or slower crop development (Anwar *et al.*, 2015; Wang *et al.*, 2017). The consequences of the rainfall biases in biophysical modelling were more complex than temperature biases because the rainfall characteristics can also alter the soil water balance and water available for plant uptake. Low rainfall intensity found in NARCliM simulations was one of the common features for RCMs (Argüeso *et al.*, 2013). Further, our analysis showed that simulated lower rainfall intensity and lower total rainfall associated with higher rainfall probability than observed climate accounted for the largest proportion of sites. Low intensity, frequent rainfall made the soil surface wetter and resulted in greater soil water distribution in shallow layers. This characteristic rainfall pattern can reduce water available for plant use because wetter soil surface can contribute more soil water evaporation, hence resulted in less water available for plant uptake. Our results showed that the responses of the wheat cropping system to this type rainfall are typically positive biases in soil evaporation across almost all sites, which consequently lead to less water available for plant transpiration and ultimately lower yield. In addition, we found that the majority of sites had negative biases in both RO and DD. This highlighted that rainfall characteristics were as important as the total amount of rainfall in agricultural systems. Improved downscaling outputs are prerequisites for realistically assessing climate change impacts in agricultural systems.

The confounding effects of RCM biases with climate change signals are an issue in the application of biophysical modelling for climate change impact assessment (e.g., Macadam *et al.*, 2016). APSIM represents the physiological process that respond to climate and soil and their interaction. In this study, the biases in NARCliM climate variables accounted for a large proportion of the APSIM biases in phenology (0.80–0.87 of R^2) and crop growth (R^2 = 0.72–0.76) (Table 2). The effects of RCM biases can overlay the climate change impacts. For example, +1 °C temperature bias resulted in negative biases in wheat flowering by −15 days, which was similar to advanced wheat flowering under future +1 °C climate warming (Anwar *et al.*, 2015). RCM biases could also subsequently lead to meaningless impact parameters or unrealistic magnitude of contribution due to climate change. This confounding of effects of the climate bias magnitude with climate change can further lead to significant collinearities between climate change and farming management practice, hence resulting in invalid regression analysis which are frequently used in determining the contribution of changes in climate change and farm managements to crop yield changes (Lobell and Burke, 2010; Liu *et al*., 2016; Liu *et al*., 2017). Therefore, climate biases can lead to false assessment of climate change impacts.

It is interesting to note that a simple SBC method applied on the modelled yield outputs could result in RCM-driven crop yields being consistent with the PDF of observation-driven crop yields. Importantly, after the SBC was applied to correct some of the biases in APSIM-simulated yield, the parameters associated with the impact assessment became more meaningful, that is, regaining positive atmospheric CO_2 effect on future crop production and diminishing the false collinearity between changes in climate variables and farm management practices. However, SBC used in our study corrects the mean and variance under the assumption of the APSIM responses of climate biases in baseline are the same as in future periods. As crop models are implemented with many linear and nonlinear functions, the response of crop models to climate biases may interact with the changes in environment conditions such as elevated future atmospheric [CO_2]. Such possible interacting responses of climate biases cannot be corrected by SBC. The SBC approach used in this study to correct the biases in biophysical modelled outputs is the same method that was used for correcting climate variables (Haerter *et al*., 2011). Undoubtedly, GCMs/RCMs-simulated climate outputs also resulted from complicated nonlinear modelling processes that are even far more complicated nonlinearity than that involved in a crop-specific biophysical modelling. The use of such a linearity of bias correction to the resultant outputs from nonlinear modelling is not ideal but provides a useful tool nevertheless. However, preferences should be given to using improved climate projections that can result in nil or little biases in biophysical modelled outputs.

Process-based crop models such as APSIM are complex biophysical models that require multiple climate variables as inputs. The realism of the relationships between these variables is important for the simulation of biophysical processes. For example, a rainy day may often be associated with lower radiation, hence lower maximum temperature and shorter diurnal temperature range than a dry day. An unrealistic combination of a dry-day's radiation with wet day, that is, with rainfall, is likely to result in higher soil water evaporation due to wet soil surface with available energy or vice versa. One advantage of dynamical downscaling, relative to many statistical downscaling methods, is that RCMs produce internally consistent data sets and maintain variable cohesiveness. However, the post-processing bias correction methods are often applied to individual climate variables separately and this can impair the spatio-temporal variable cohesiveness and consistency in the climate data (Ehret *et al*., 2012; Teutschbein and Seibert, 2013). The consequence of using the resultant climate data to run biophysical models can result in substantial errors in the modelled outputs and can further complicate the crop modelling through interacting with farm management options. This is because soil nutrient uptake depends on water uptake, negative bias in soil water uptake can restrict up-taking abundant nitrogen available in the soils hence enlarge the consequence of RCM biases on crop growth. Soil water is the centre of nearly all soil biological and chemical activities. Hence, the effectiveness of farm management options such as residue incorporation and nitrogen applications are largely influenced by soil water, meaning the rainfall is the primary factor for achieving realistic modelling outputs in a semiarid environment. Therefore, improved downscaled rainfall is a crucial step for realistic assessment of climate change impacts in agricultural systems.

5 | CONCLUSIONS

For the NARCliM bias-corrected data, we conducted comprehensive analysis of residual biases for different crop growing stages and quantitatively determined the impacts on crop model outputs. Substantial biases were identified in the NARCliM data for the crop growing season. The growing season temperature bias was translated to delay or advance crop phenology when used as inputs for APSIM simulation. The biases in rainfall characteristics were generally positive in rainfall probability and negative in rainfall intensity, which resulted in APSIM-simulated negative biases for most of the study area in RO and DD and positive bias in soil evaporation. Consequently, biases in soil water balance and water availability resulted in less plant transpiration and less N uptake. Ultimately, those biases together with biases in crop phenology led to biases in crop yields. In addition, crop management options particularly N applications could interact with biases in RCM-simulated climate variables. This study suggests that existing bias correction of NARCliM climate data does not result in climate data that can be used for the assessment of climate change in agricultural studies. Therefore, it is desirable to use more sophisticated post bias correction technique on RCM climate data for realistic assessments of climate change impacts in agricultural systems.

Our study highlights that for assessing crop production, the fundament importance of firstly assessing the biases and uncertainties of climate projections and testing the hypothesis of whether the outputs of biophysical models driven by GCMs/RCMs-simulated climate are identical to those driven by observed climate. SBC should be applied to correct the biases in biophysical modelled outputs for realistic assessment of climate change impacts. However, because the SBC has limitations in correcting the nonlinearity of biophysical responses to climate biases, preferences should be given to using improved climate projections that can result in little biases in biophysical modelled outputs.

ACKNOWLEDGEMENTS

This work was supported by NSW Department of Primary Industries and partially funded by NSW Office of Environment and Heritage (OEH) for the project entitled "Assessment of climate change impacts on major crops and identification of farming management option in southern NSW" (RDE959) as a part of the Climate Change Fund supported research led by OEH.

ORCID

De Li Liu https://orcid.org/0000-0003-2574-1908
Bin Wang https://orcid.org/0000-0002-6422-5802

REFERENCES

Anwar, M.R., Liu, D.L., Farquharson, R., Macadam, I., Abadi, A., Finlayson, J., Wang, B. and Ramilan, T. (2015) Climate change impacts on phenology and yields of five broadacre crops at four climatologically distinct locations in Australia. *Agricultural Systems*, 132, 133–144.

Argüeso, D., Evans, J. and Fita, L. (2013) Precipitation bias correction of very high resolution regional climate models. *Hydrology and Earth System Sciences*, 17, 4379–4388.

Bakker, A.M.R., Bessembinder, J.J.E., de Wit, A.J.W., van den Hurk, B.J.J.M. and Hoek, S.B. (2014) Exploring the efficiency of bias corrections of regional climate model output for the assessment of future crop yields in Europe. *Regional Environmental Change*, 14, 865–877.

Cammarano, D., Rivington, M., Matthews, K.B., Miller, D.G. and Bellocchi, G. (2017) Implications of climate model biases and downscaling on crop model simulated climate change impacts. *European Journal of Agronomy*, 88, 63–75.

Di Luca, A., Argüeso, D., Evans, J.P., Elía, R. and Laprise, R. (2016) Quantifying the overall added value of dynamical downscaling and the contribution from different spatial scales. *Journal of Geophysical Research: Atmospheres*, 121, 1575–1590.

Di Luca, A., Evans, J.P. and Ji, F. (2018) Australian snowpack in the NARCliM ensemble: evaluation, bias correction and future projections. *Climate Dynamics*, 51, 639–666.

Doetterl, S., Stevens, A., Six, J., Merckx, R., Van Oost, K., Pinto, M.C., Casanova-Katny, A., Muñoz, C., Boudin, M. and Venegas, E.Z. (2015) Soil carbon storage controlled by interactions between geochemistry and climate. *Nature Geoscience*, 8, 780–783.

Donatelli, M., Srivastava, A.K., Duveiller, G., Niemeyer, S. and Fumagalli, D. (2015) Climate change impact and potential adaptation strategies under alternate realizations of climate scenarios for three major crops in Europe. *Environmental Research Letters*, 10, 075005.

Ehret, U., Zehe, E., Wulfmeyer, V., Warrach-Sagi, K. and Liebert, J. (2012) HESS opinions "Should we apply bias correction to global and regional climate model data?". *Hydrology and Earth System Sciences*, 16, 3391–3404.

Evans, J.P., Ekström, M. and Ji, F. (2012) Evaluating the performance of a WRF physics ensemble over south-east Australia. *Climate Dynamics*, 39, 1241–1258.

Evans, J., Ji, F., Lee, C., Smith, P., Argüeso, D. and Fita, L. (2014) Design of a regional climate modelling projection ensemble experiment–NARCliM. *Geoscientific Model Development*, 7, 621–629.

Evans, J.P., Argueso, D., Olson, R. and Di Luca, A. (2017) Bias-corrected regional climate projections of extreme rainfall in south-east Australia. *Theoretical and Applied Climatology*, 130, 1085–1098.

Fita, L., Evans, J.P., Argüeso, D., King, A. and Liu, Y. (2017) Evaluation of the regional climate response in Australia to large-scale climate modes in the historical NARCliM simulations. *Climate Dynamics*, 49, 2815–2829.

Fowler, H., Blenkinsop, S. and Tebaldi, C. (2007) Linking climate change modelling to impacts studies: recent advances in downscaling techniques for hydrological modelling. *International Journal of Climatology*, 27, 1547–1578.

Giorgi, F., Hewitson, B., Christensen, J., Hulme, M., Von Storch, H., Whetton, P., Jones, R., Mearns, L., Fu, C. and Arritt, R. (2001) Regional climate information—evaluation and projections. In: Ding, Y. , Griggs, D.J. , Noguer, M. , van der Linden, P.J. , Dai, X. , Maskell, K. and Johnson, C.A. (Eds.) *Climate Change 2001: The Scientific Basis. Contribution of Working Group I to the Third Assessment Report of the Intergovernmental Panel on Climate Change*. Cambridge and New York, NY: Cambridge University Press.

Glotter, M., Elliott, J., McInerney, D., Best, N., Foster, I. and Moyer, E.J. (2014) Evaluating the utility of dynamical downscaling in agricultural impacts projections. *Proceedings of the National Academy of Sciences of the United States of America*, 111, 8776–8781.

Haerter, J., Hagemann, S., Moseley, C. and Piani, C. (2011) Climate model bias correction and the role of timescales. *Hydrology and Earth System Sciences*, 15, 1065–1079.

Holzworth, D.P., Huth, N.I., deVoil, P.G., Zurcher, E.J., Herrmann, N.I., McLean, G., Chenu, K., van Oosterom, E.J., Snow, V., Murphy, C., Moore, A.D., Brown, H., Whish, J.P.M., Verrall, S., Fainges, J., Bell, L.W., Peake, A.S., Poulton, P.L., Hochman, Z., Thorburn, P.J., Gaydon, D.S., Dalgliesh, N.P., Rodriguez, D., Cox, H., Chapman, S., Doherty, A., Teixeira, E., Sharp, J., Cichota, R., Vogeler, I., Li, F.Y., Wang, E., Hammer, G.L., Robertson, M.J., Dimes, J.P., Whitbread, A.M., Hunt, J., van Rees, H., McClelland, T., Carberry, P.S., Hargreaves, J.N.G., MacLeod, N., McDonald, C., Harsdorf, J., Wedgwood, S. and Keating, B.A. (2014) APSIM—evolution towards a new generation of agricultural systems simulation. *Environmental Modelling & Software*, 62, 327–350.

Isbell, R. (2016) *The Australian Soil Classification*. Clayton South Vic, Australia: CSIRO Publishing.

Jeffrey, S.J., Carter, J.O., Moodie, K.B. and Beswick, A.R. (2001) Using spatial interpolation to construct a comprehensive archive of Australian climate data. *Environmental Modelling & Software*, 16, 309–330.

Ji, F., Ekström, M., Evans, J.P. and Teng, J. (2014) Evaluating rainfall patterns using physics scheme ensembles from a regional atmospheric model. *Theoretical and Applied Climatology*, 115, 297–304.

Ji, F., Evans, J.P., Argueso, D., Fita, L. and Di Luca, A. (2015) Using large-scale diagnostic quantities to investigate change in East Coast Lows. *Climate Dynamics*, 45, 2443–2453.

Ji, F., Remenyi, T., Harris, R., Evans, J., Di Lucac, A. and Beyera, K. (2018) Projected changes in frequency of suitable snowmaking conditions for the Australian Alps. In: *22nd International Congress on Modelling and Simulation, Hobart, Tasmania, Australia, 3–8 December 2017.*

Jin, J., Wang, S.-Y. and Gillies, R.R. (2011) An improved dynamical downscaling for the western United States. In J. Blanco, and H. Kheradmand, (Eds.), *Climate Change-Research and Technology for Adaptation and Mitigation*. Janeza Trdine, Rijeka, Croatia: InTech.

Jones, D.A., Wang, W. and Fawcett, R. (2009) High-quality spatial climate data-sets for Australia. *Australian Meteorological and Oceanographic Journal*, 58, 233–248.

Keating, B.A., Carberry, P.S., Hammer, G.L., Probert, M.E., Robertson, M.J., Holzworth, D., Huth, N.I., Hargreaves, J.N., Meinke, H. and Hochman, Z. (2003) An overview of APSIM, a model designed for farming systems simulation. *European Journal of Agronomy*, 18, 267–288.

Liu, D.L., O'Leary, G.J., Ma, Y., Cowie, A., Li, F.Y., McCaskill, M., Conyers, M., Dalal, R., Robertson, F. and Dougherty, W. (2016) Modelling soil organic carbon 2. Changes under a range of cropping and grazing farming systems in eastern Australia. *Geoderma*, 265, 164–175.

Liu, D.L., Zeleke, K.T., Wang, B., Macadam, I., Scott, F. and Martin, R.J. (2017) Crop residue incorporation can mitigate negative climate change impacts on crop yield and improve water use efficiency in a semiarid environment. *European Journal of Agronomy*, 85, 51–68.

Lobell, D.B. and Burke, M.B. (2010) On the use of statistical models to predict crop yield responses to climate change. *Agricultural and Forest Meteorology*, 150, 1443–1452.

Macadam, I., Argüeso, D., Evans, J.P., Liu, D.L. and Pitman, A.J. (2016) The effect of bias correction and climate model resolution on wheat simulations forced with a regional climate model ensemble. *International Journal of Climatology*, 36, 4577–4591.

Manage, N.P., Lockart, N., Willgoose, G., Kuczera, G., Kiem, A.S., Chowdhury, A.K., Zhang, L. and Twomey, C. (2016) Statistical testing of dynamically downscaled rainfall data for the Upper Hunter region, New South Wales, Australia. *Journal of Southern Hemisphere Earth Systems Science*, 66, 203–227.

O'Leary, G.J., Liu, D.L., Ma, Y., Li, F.Y., McCaskill, M., Conyers, M., Dalal, R., Reeves, S., Page, K., Dang, Y.P. and Robertson, F. (2016) Modelling soil organic carbon 1. Performance of APSIM crop and pasture modules against long-term experimental data. *Geoderma*, 264(Part A), 227–237.

Olson, R., Fan, Y. and Evans, J.P. (2016a) A simple method for Bayesian model averaging of regional climate model projections: application to southeast Australian temperatures. *Geophysical Research Letters*, 43, 7661–7669.

Olson, R., Evans, J.P., Di Luca, A. and Argüeso, D. (2016b) The NARCliM project: model agreement and significance of climate projections. *Climate Research*, 69, 209–227.

Pandey, V., Sharma, M., Deeba, F., Maurya, V.K., Gupta, S.K., Singh, S.P., Mishra, A. and Nautiyal, C.S. (2017) Impact of elevated CO_2 on wheat growth and yield under free air CO_2 enrichment. *American Journal of Climate Change*, 6, 573–596.

Pascal, O., Benjamin, S., Christian, B. and Mathieu, V. (2011) Are regional climate models relevant for crop yield prediction in West Africa? *Environmental Research Letters*, 6, 014008.

Piani, C., Haerter, J. and Coppola, E. (2010) Statistical bias correction for daily precipitation in regional climate models over Europe. *Theoretical and Applied Climatology*, 99, 187–192.

Ramarohetra, J., Pohl, B. and Sultan, B. (2015) Errors and uncertainties introduced by a regional climate model in climate impact assessments: example of crop yield simulations in West Africa. *Environmental Research Letters*, 10, 124014.

Ruiz-Ramos, M. and Mínguez, M.I. (2010) Evaluating uncertainty in climate change impacts on crop productivity in the Iberian Peninsula. *Climate Research*, 44, 69–82.

Ruiz-Ramos, M., Rodríguez, A., Dosio, A., Goodess, C.M., Harpham, C., Mínguez, M.I. and Sánchez, E. (2016) Comparing correction methods of RCM outputs for improving crop impact projections in the Iberian Peninsula for 21st century. *Climatic Change*, 134, 283–297.

Skamarock, W.C., Klemp, J.B., Dudhia, J., Gill, D.O., Barker, D.M., Wang, W. and Powers, J.G. (2005) *A description of the advanced research WRF version 2*. Boulder, CO: National Center For Atmospheric Research.

Stine, R.A. (1995) Graphical interpretation of variance inflation factors. *The American Statistician*, 49, 53–56.

Teutschbein, C. and Seibert, J. (2013) Is bias correction of regional climate model (RCM) simulations possible for non-stationary conditions? *Hydrology and Earth System Sciences*, 17, 5061–5077.

Vanuytrecht, E., Raes, D., Willems, P. and Semenov, M.A. (2014) Comparing climate change impacts on cereals based on CMIP3 and EU-ENSEMBLES climate scenarios. *Agricultural and Forest Meteorology*, 195, 12–23.

Wang, B., Chen, C., Liu, D.L., Asseng, S., Yu, Q. and Yang, X. (2015) Effects of climate trends and variability on wheat yield variability in eastern Australia. *Climate Research*, 64, 173–186.

Wang, B., Liu, D.L., Asseng, S., Macadam, I., Yang, X. and Yu, Q. (2017) Spatiotemporal changes in wheat phenology, yield and water use efficiency under the CMIP5 multimodel ensemble projections in eastern Australia. *Climate Research*, 72, 83–99.

Wiebe, K., Lotze-Campen, H., Sands, R., Tabeau, A., van der Mensbrugghe, D., Biewald, A., Bodirsky, B., Islam, S., Kavallari, A. and Mason-D'Croz, D. (2015) Climate change impacts on agriculture in 2050 under a range of plausible socioeconomic and emissions scenarios. *Environmental Research Letters*, 10, 085010.

Xu, Z. and Yang, Z.-L. (2012) An improved dynamical downscaling method with GCM bias corrections and its validation with 30 years of climate simulations. *Journal of Climate*, 25, 6271–6286.

Yang, Y., Liu, D.L., Anwar, M.R., Zuo, H. and Yang, Y. (2014) Impact of future climate change on wheat production in relation to plant-available water capacity in a semiarid environment. *Theoretical and Applied Climatology*, 115, 391–410.

Yang, X., Yu, B., Zhu, Q. and Liu, D.L. (2016a) Predicting changes of rainfall erosivity and hillslope erosion across New South Wales, Australia. *Journal of Earth Science and Climate Change*, 7, 340. https://doi.org/10.4172/2157-7617.1000340.

Yang, Y., Liu, D.L., Anwar, M.R., O'Leary, G., Macadam, I. and Yang, Y. (2016b) Water use efficiency and crop water balance of rainfed wheat in a semi-arid environment: sensitivity of future changes to projected climate changes and soil type. *Theoretical and Applied Climatology*, 123, 565–579.

Yin, C., Li, Y., Ye, W., Bornman, J.F. and Yan, X. (2011) Statistical downscaling of regional daily precipitation over southeast Australia based on self-organizing maps. *Theoretical and Applied Climatology*, 105, 11–26.

How to cite this article: Liu DL, Wang B, Evans J, *et al.* Propagation of climate model biases to biophysical modelling can complicate assessments of climate change impact in agricultural systems. *Int J Climatol*. 2019;39:424–444. https://doi.org/10.1002/joc.5820